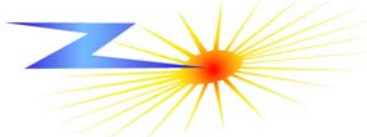




SAND2007-2058C



Implosion Energetics via Analysis of Mass Density Profile Evolution and Spectrally-Resolved Imaging

Brent Jones
Sandia National Laboratories

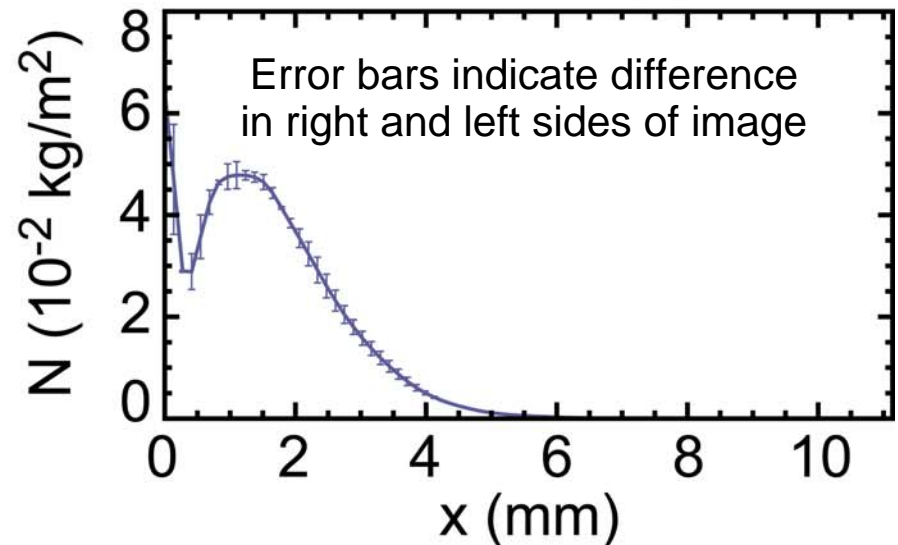
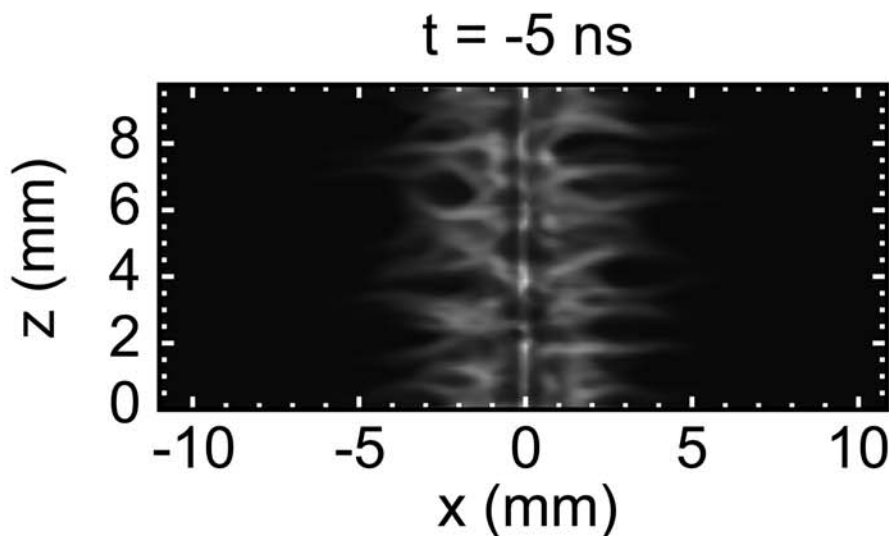
2007 Wire Array Workshop
Battle, UK – April 2-5, 2007

Overview



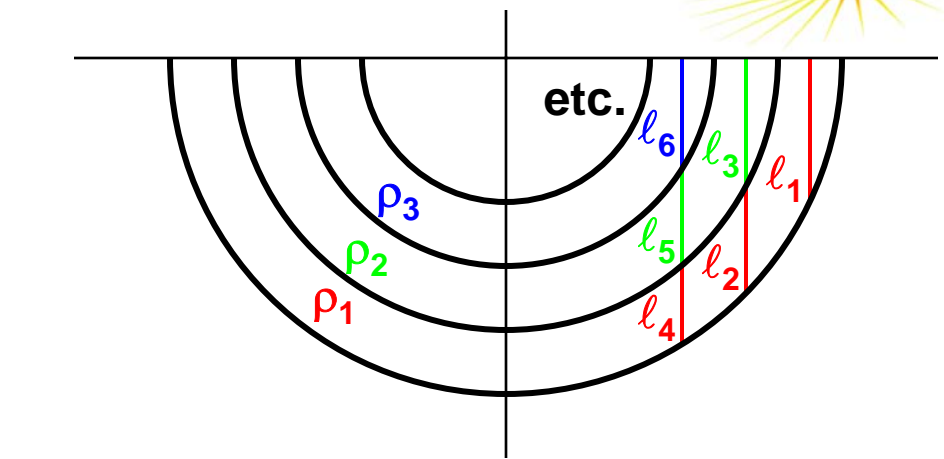
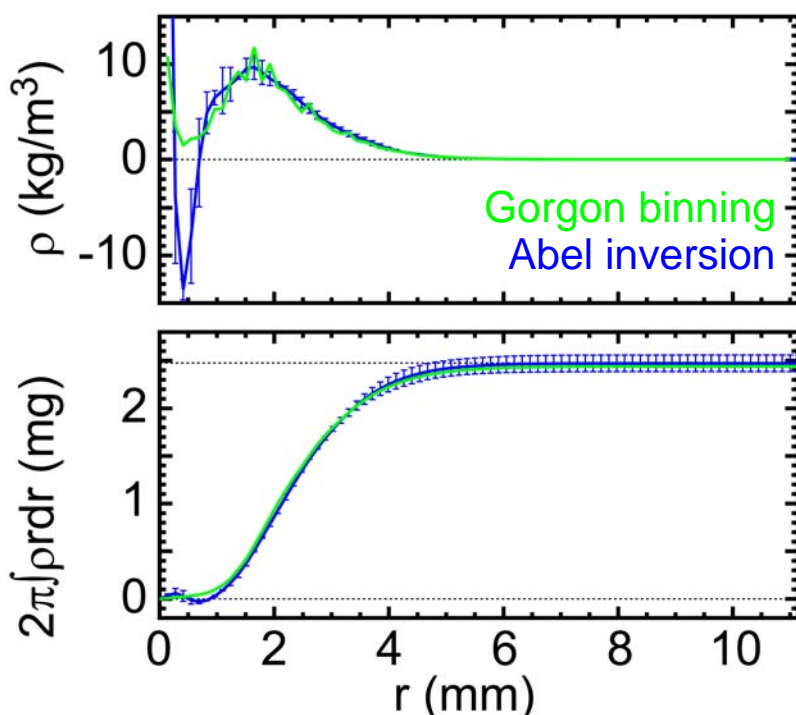
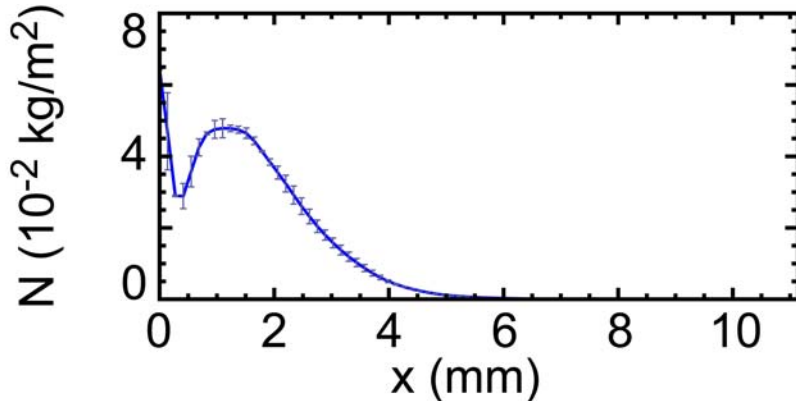
- How much information can we obtain through observation of the mass density profile evolution during z-pinch implosion?
 - Abel inversion of imaging data
 - Continuity equation analysis to obtain kinetic energy
- How can we measure $\rho(r,t)$ experimentally?
 - Multi-frame x-ray radiography
 - Time-resolved x-ray self-emission diagnostics
- K-shell spectroscopy of low-Z wire arrays
 - Doppler shift measurements can give velocity
 - Plasma parameters inferred in different regions, particularly on-axis where Abel inversion is most problematic

2D areal density images from 3D MHD simulation (Jennings)



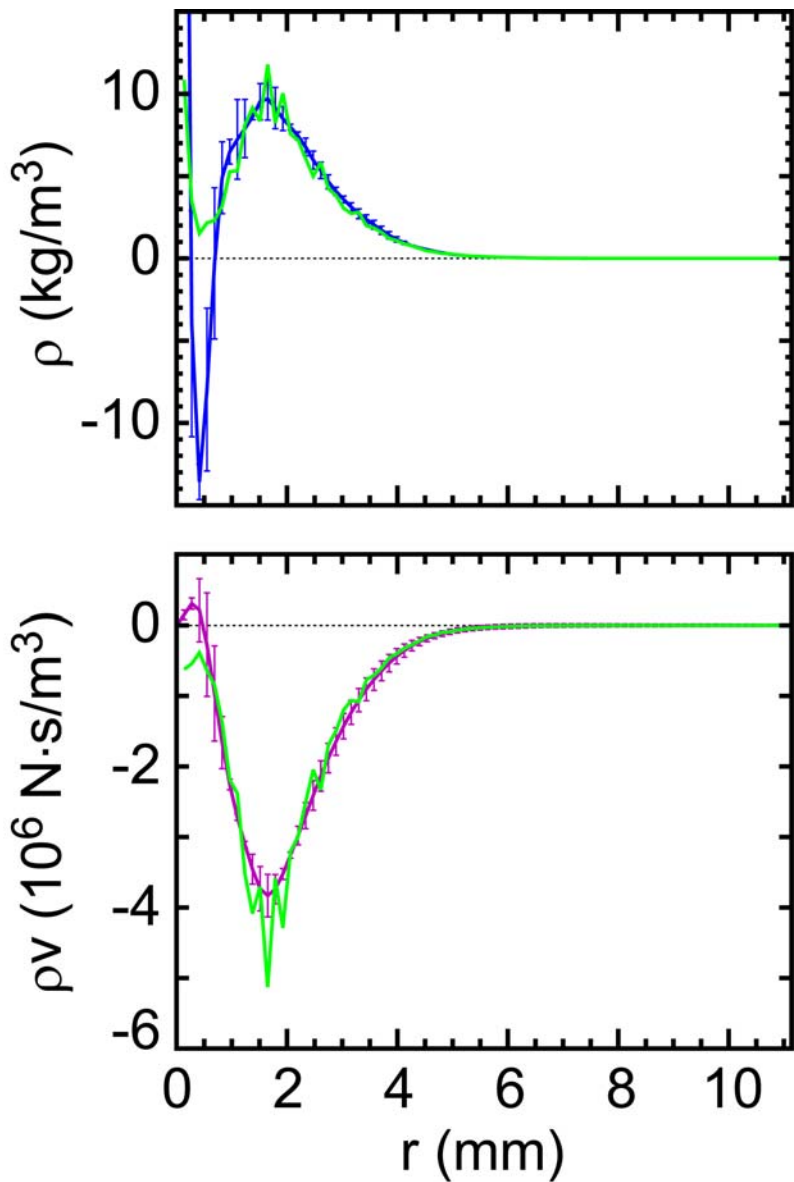
- 3D MHD Gorgon code, circuit model with shunting resistor
- 2.5 mg W wire array, 20 mm initial diameter, 120 wires, *ad hoc* perturbations to seed implosion instabilities
- 2D areal density map generated every 1 ns
- Center of image found by minimizing RMS difference between left and right sides
- Image is axially and left-right averaged to produce line-integrated density $N(x)$

Mass density profile from onion-peeling Abel inversion



- Assumes cylindrical symmetry
- Numerical Abel inversion method
 - B. Jones *et al.*, IEEE T. Plasma Sci, **34**, 213 (2006).
- Onion-peeling does not handle noisy images well, but adequate for this case
- Average mass density profile from code calculated by summing xyz points in radial bins

Momentum density profile inferred from continuity equation



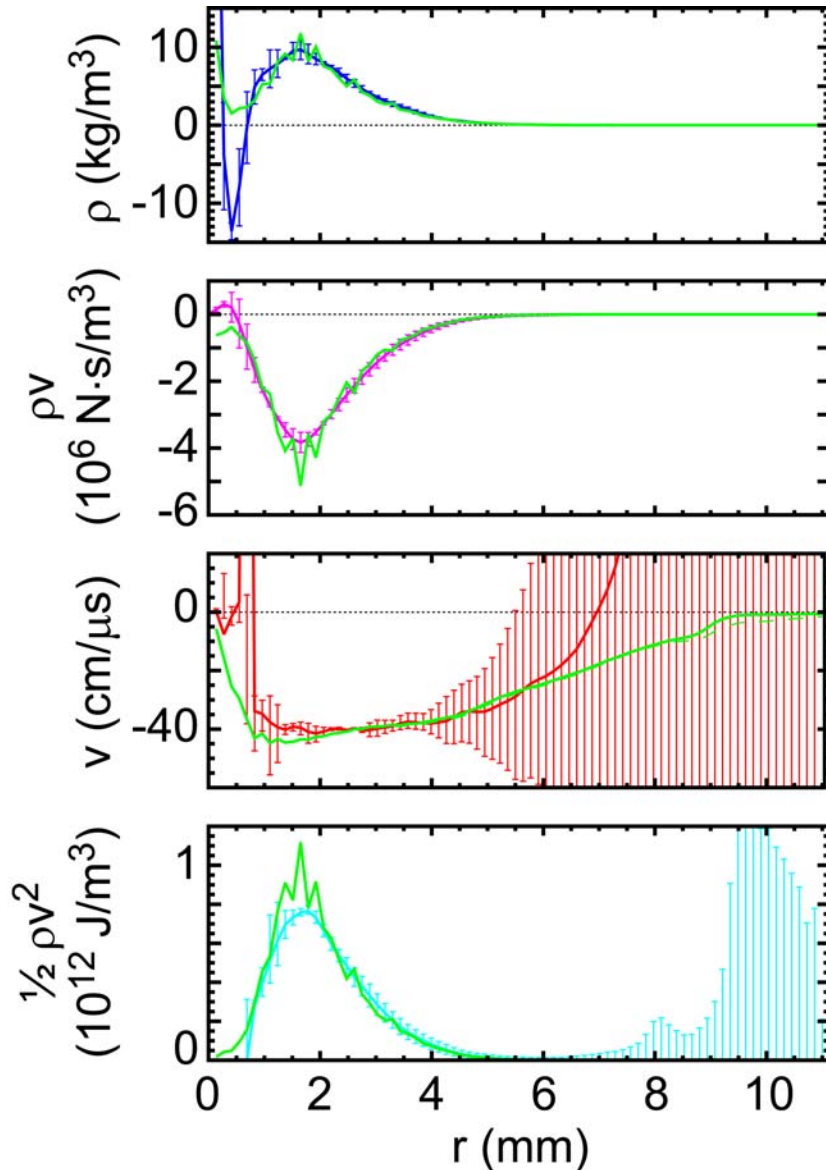
$$\frac{\partial \rho}{\partial t} + \nabla \cdot (\rho \vec{v}) = 0$$

$$\frac{\partial \rho}{\partial t} + \frac{1}{r} \frac{\partial}{\partial r} (r \rho v) = 0$$

$$\rho v = - \frac{1}{r} \int_0^r \frac{\partial \rho}{\partial t} r dr$$

- Assumes cylindrical symmetry with only radial motion
- Derivative in integrand calculated numerically from linear fit to three time points in $\rho(r,t)$ matrix
- Integration performed numerically over discrete r values

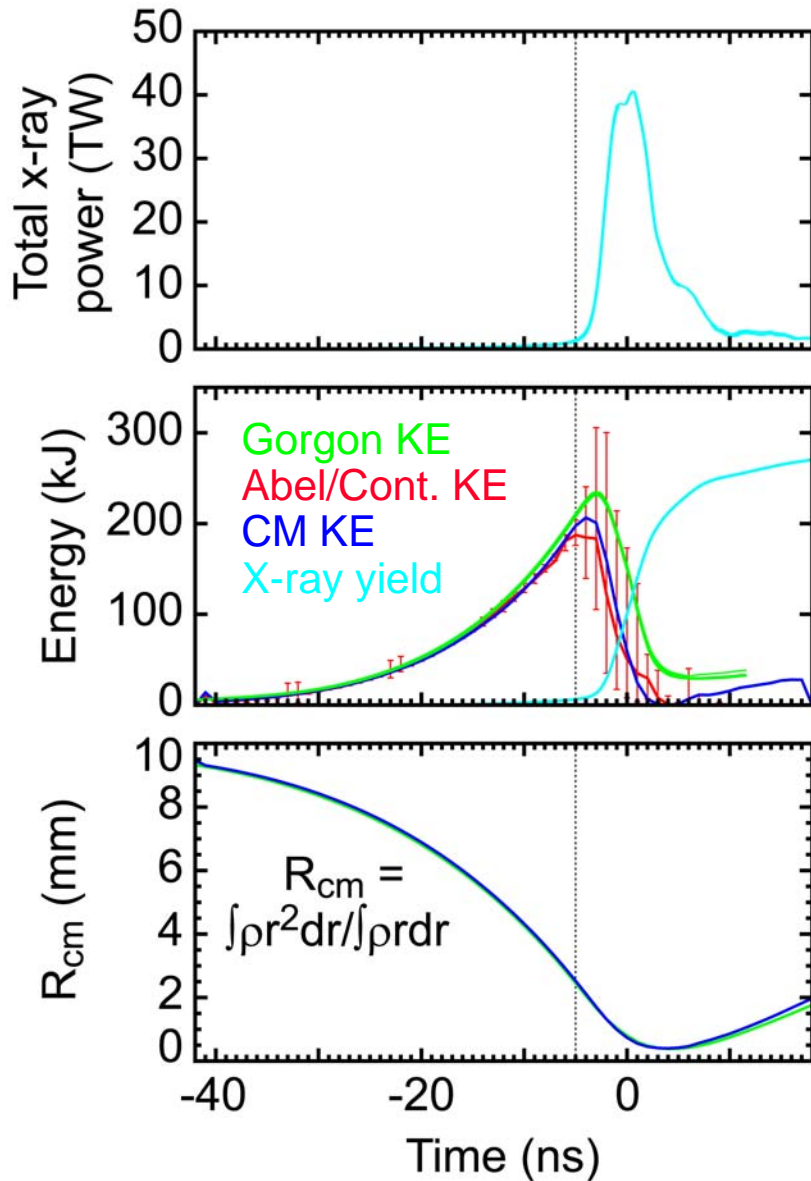
Velocity and kinetic energy profiles from ρ and ρv profiles



$$v = \frac{1}{\rho} \rho v$$
$$k = \frac{1}{2} \frac{(\rho v)^2}{\rho}$$

- Average kinetic energy density profile from code calculated by summing xyz points in radial bins
- Average velocity profile from code is from $v = \sqrt{2k/\rho}$
- $k(r)$ is valid except where ρ is very low; $1/\rho$ factor leads to errors

Comparison of kinetic energy evolution



- Integrate $k(r)$ to get $KE(t)$
 - Remove points with $\rho < 0.05 \rho_{\max}$ to avoid division by low numbers
- Compares well with Gorgon KE until just before peak KE
 - Abel inversion problems near the axis
 - Could be a lot of azimuthal non-uniformity (note right-left discrepancy)
 - Need to check if flow has azimuthal component near stagnation
 - Note early time discrete wire structures leads to Abel artifacts
- Velocity of the center of mass gives equivalent KE
 - All mass moving at nearly same velocity



Sandia
National
Laboratories

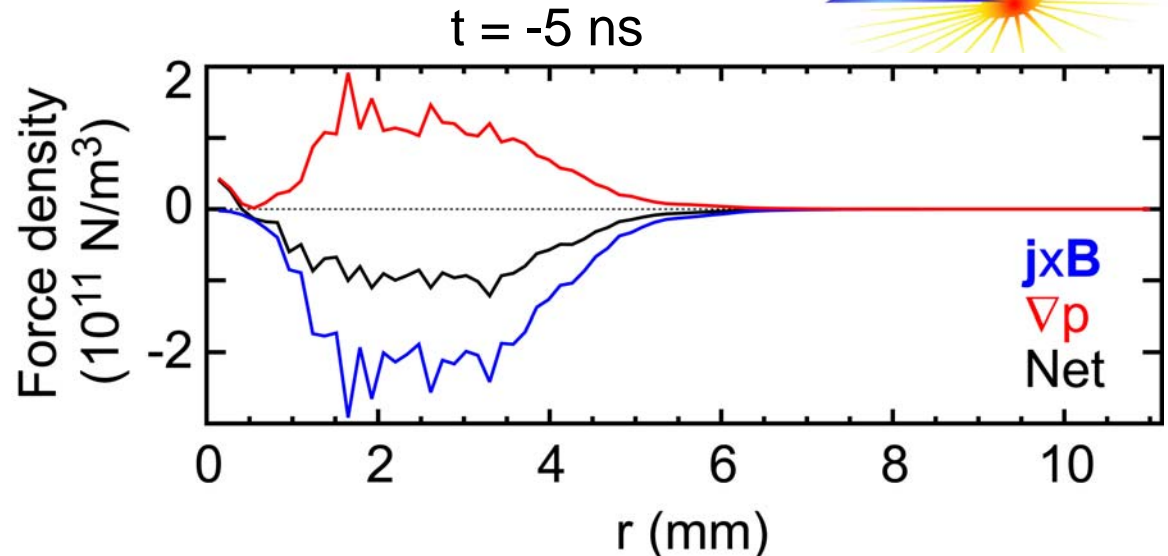
Other energetics considerations near stagnation



Force density from momentum equation

$$f = \rho \left(\frac{\partial}{\partial t} + \vec{v} \cdot \nabla \right) \vec{v}$$

$$= \rho \left(\frac{\partial}{\partial t} + v \frac{\partial}{\partial r} \right) v$$



Compressional p·dV heating driven by $j \times B$ during deceleration/stagnation phase

$$\frac{\partial}{\partial t} (e_{\text{int}} + k)_{p \cdot dV} = -\nabla \cdot (p \vec{v})$$

$$= -\frac{1}{r} \frac{\partial}{\partial r} (r p v)$$

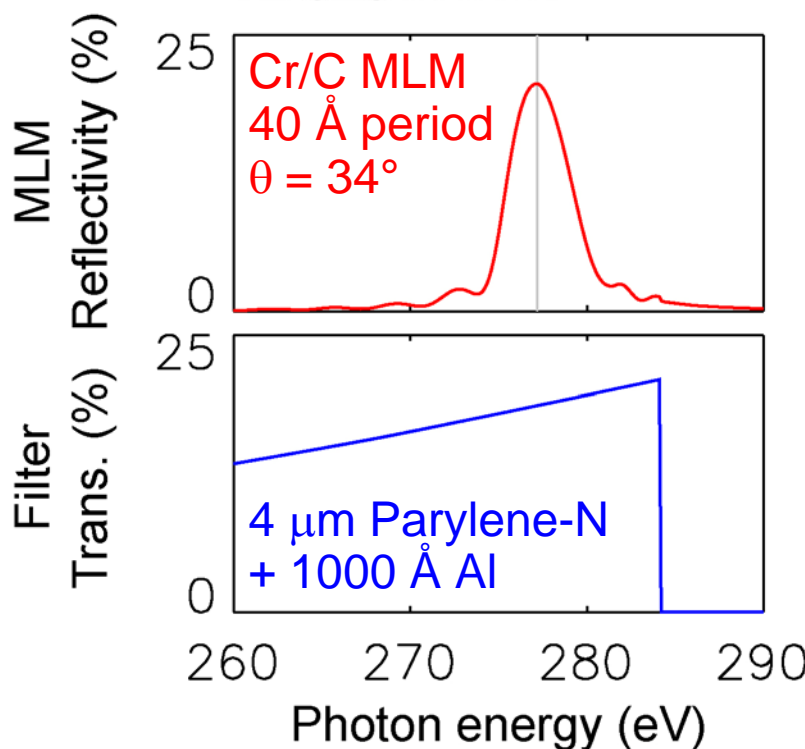
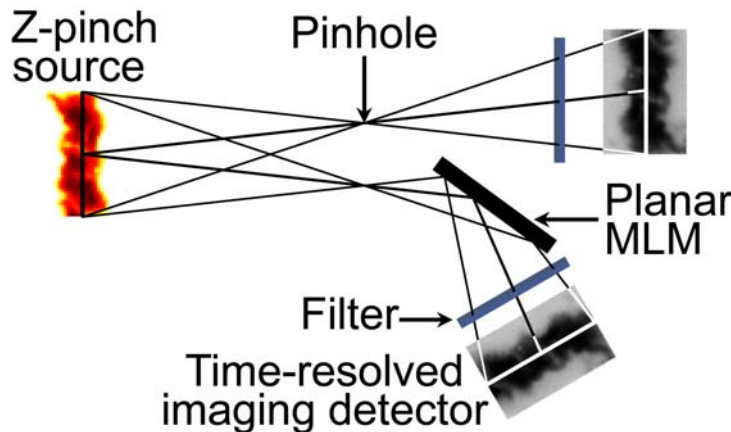
$$p = n_e T_e + n_i T_i$$

- From Gorgon, ∇p force balances $j \times B$ force near stagnation
- Plasma decelerates but $j \times B$ can continue to do work
- Can we infer a strong ∇p from force density via $p(r,t)$?
- Would need v , n , T profiles to infer $p \cdot dV$ work



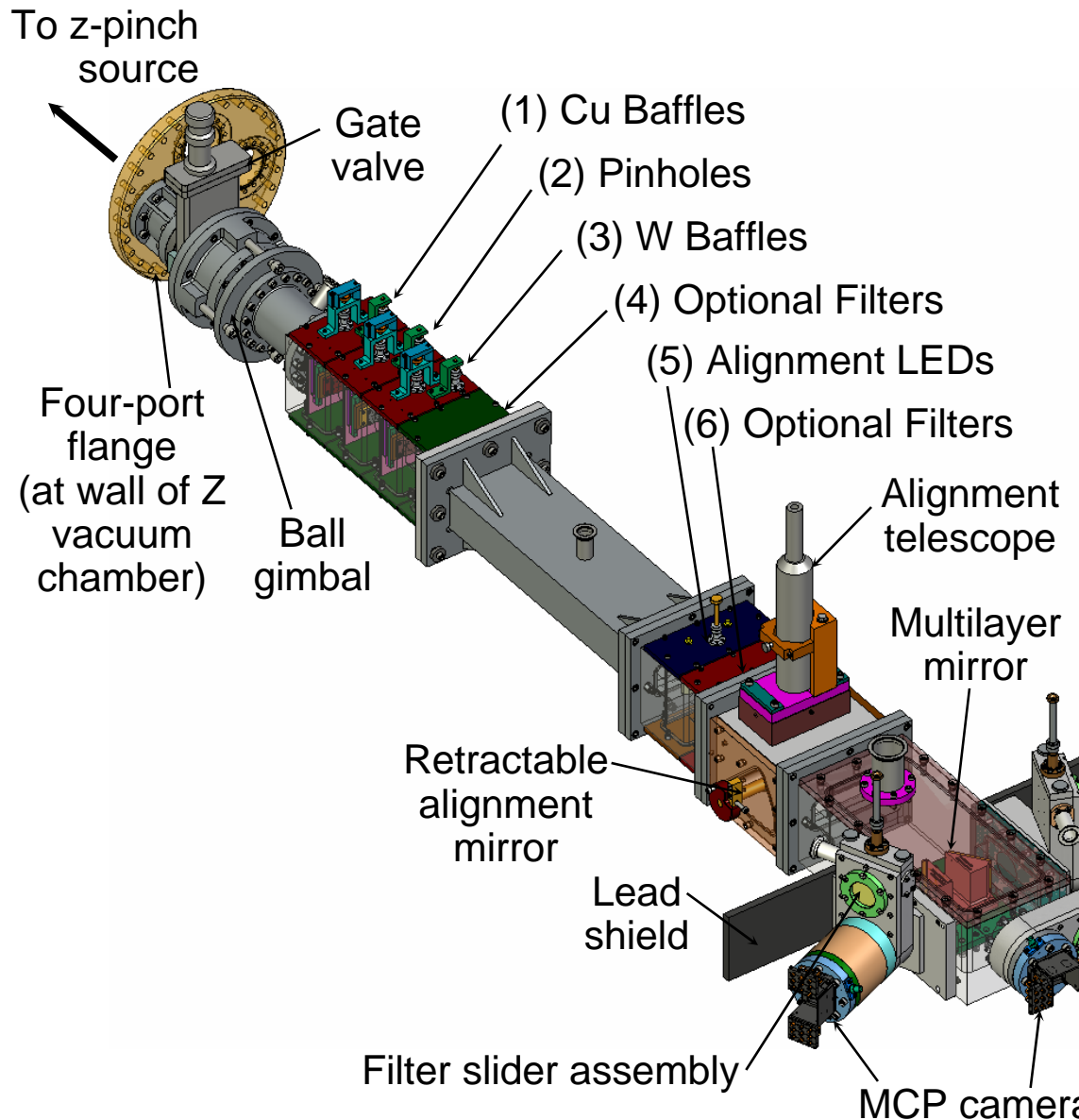
Sandia
National
Laboratories

MLM pinhole camera produces monochromatic images



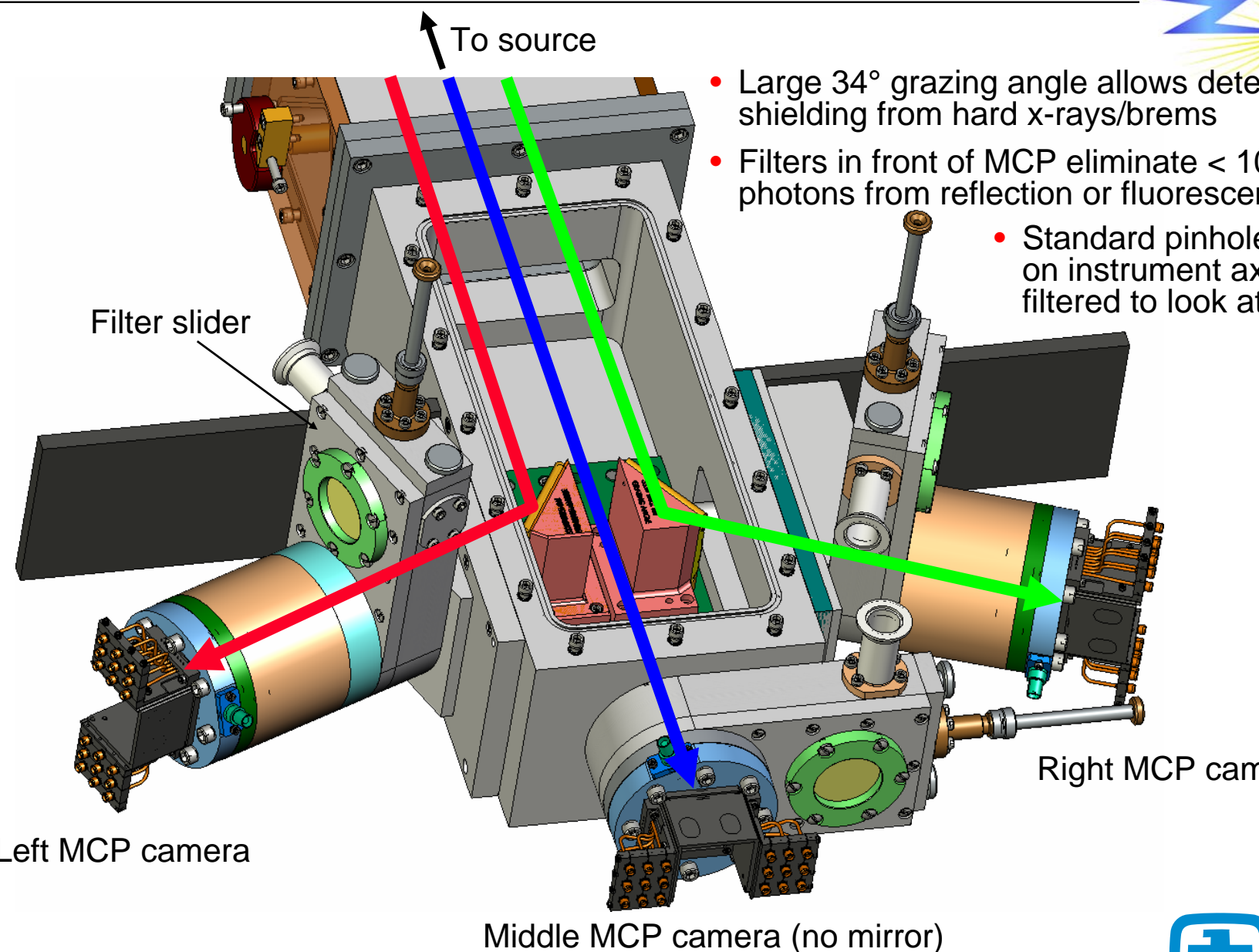
- Pinhole images are reflected from planar Cr/C multilayer mirror (MLM)
 - Calculated 20% peak reflectivity, ~5 eV photon energy bandwidth
 - 34° grazing angle allows shielding of detector from hard x-rays
- Thin filter blocks UV/visible light, suppresses second harmonic MLM reflection
- Instrument on the Z machine combines MLM-reflected and standard pinhole cameras (PHC)

MLM pinhole imager has been fielded on the Z accelerator



- Instrument mounts on 12° side-on LOS
- 3 PHCs can be fielded (one without mirror reflection)
- Ball gimble pivots to align with source
- Alignment under vacuum corrects for pipe sag and movement in Z load region
- Instrument is differentially pumped behind gate valve

Three simultaneous 8-frame MCPs are now built for Z imager



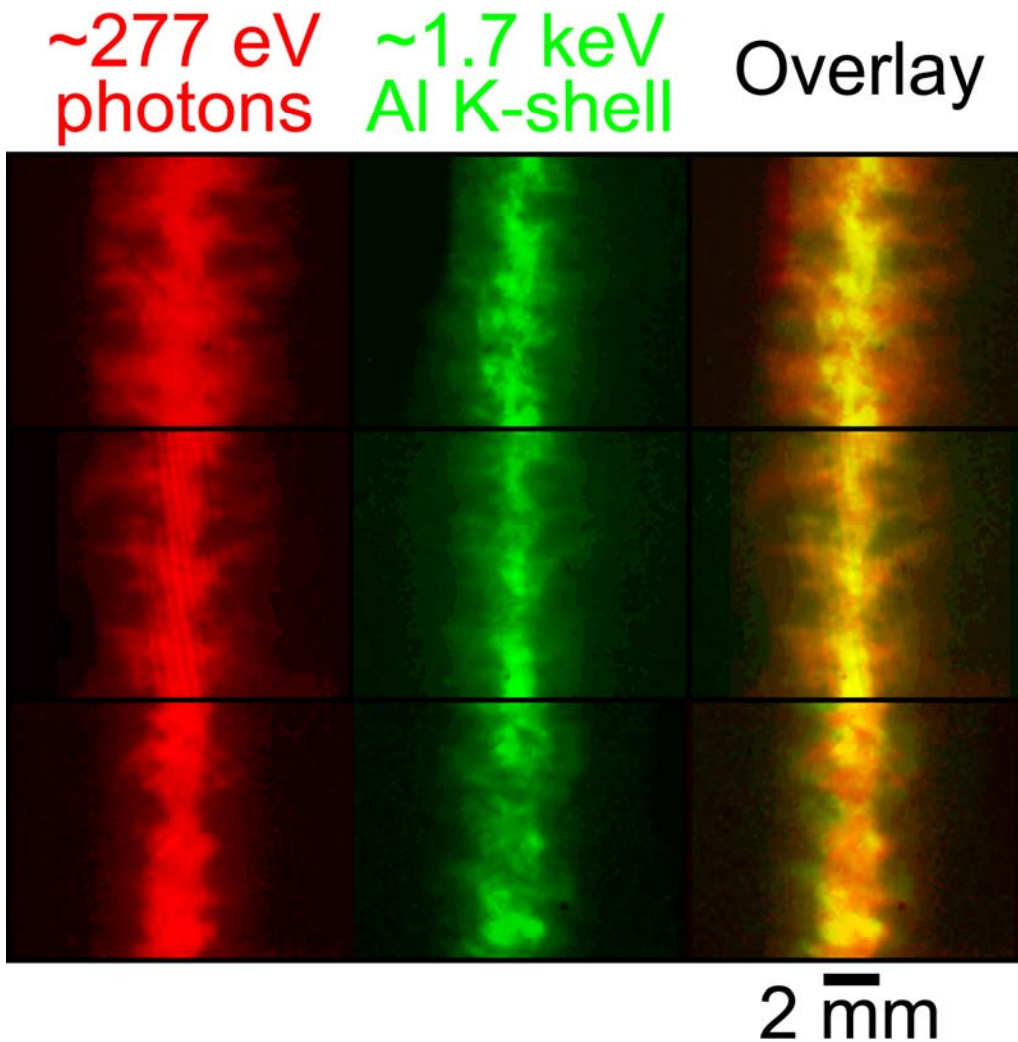
- Large 34° grazing angle allows detector shielding from hard x-rays/brems
- Filters in front of MCP eliminate < 100 eV photons from reflection or fluorescence at MLM
- Standard pinhole camera on instrument axis can be filtered to look at >1 keV



Sandia
National
Laboratories

BJ 11

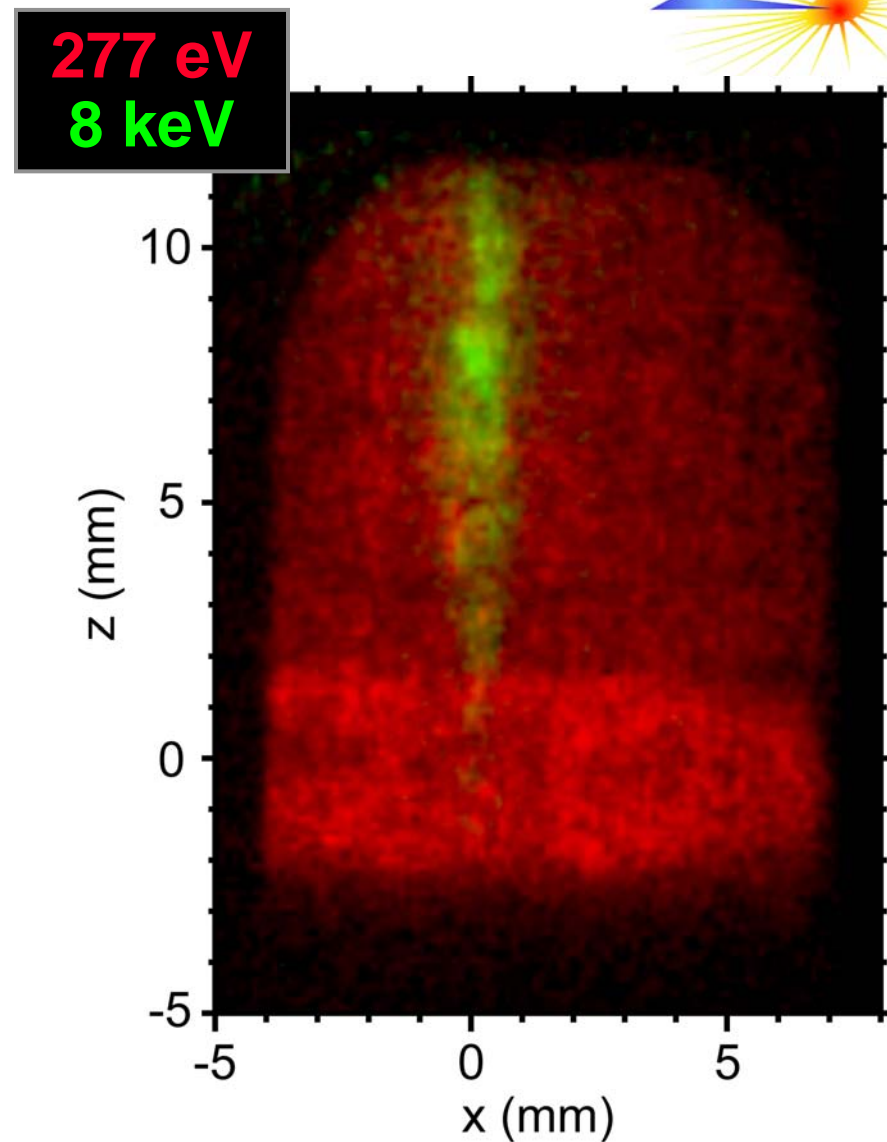
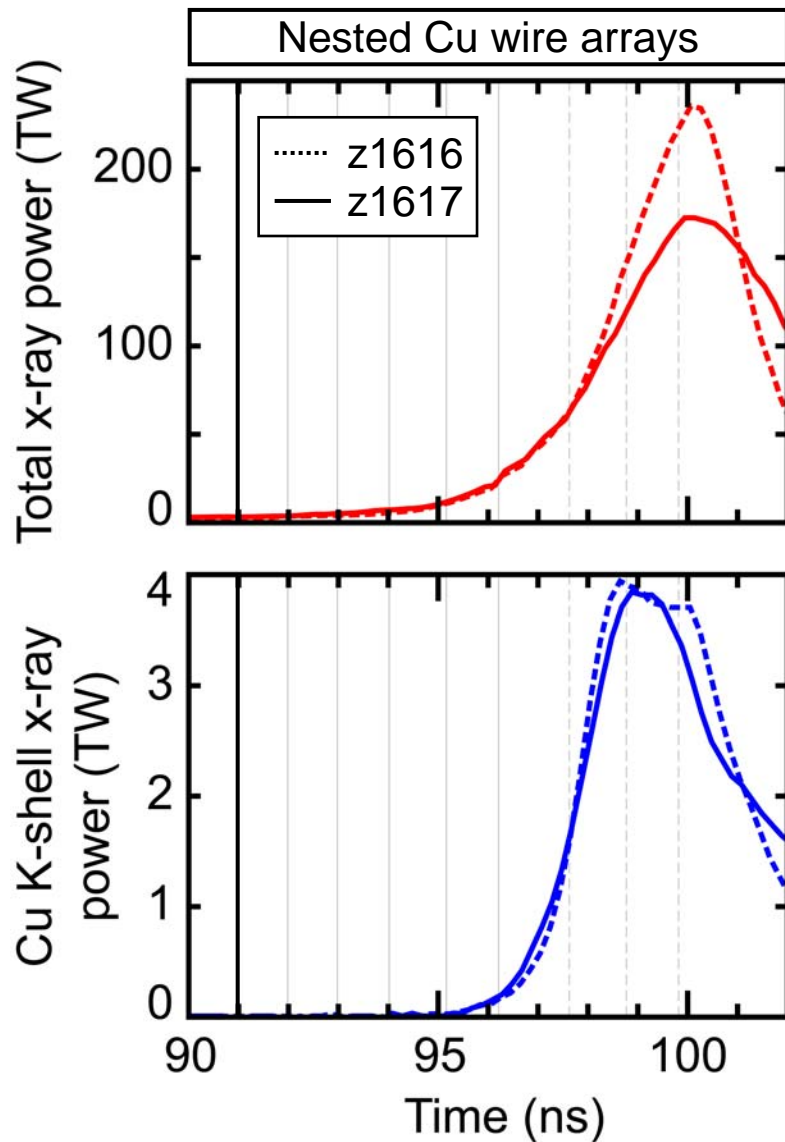
Z-pinch implosion structure imaged at multiple energies



- Nested Al wire array z pinch
- Simultaneous imaging at two photon energies
- Imploding fingers of trailing cooler mass in ~277 eV images
- Al K-shell emitted from hot, dense column accreting on axis

- Opaque regions of cool plasma mask core after peak x-rays
- Striations on ~277 eV frame at -0.3 ns apparently due to MLM defect

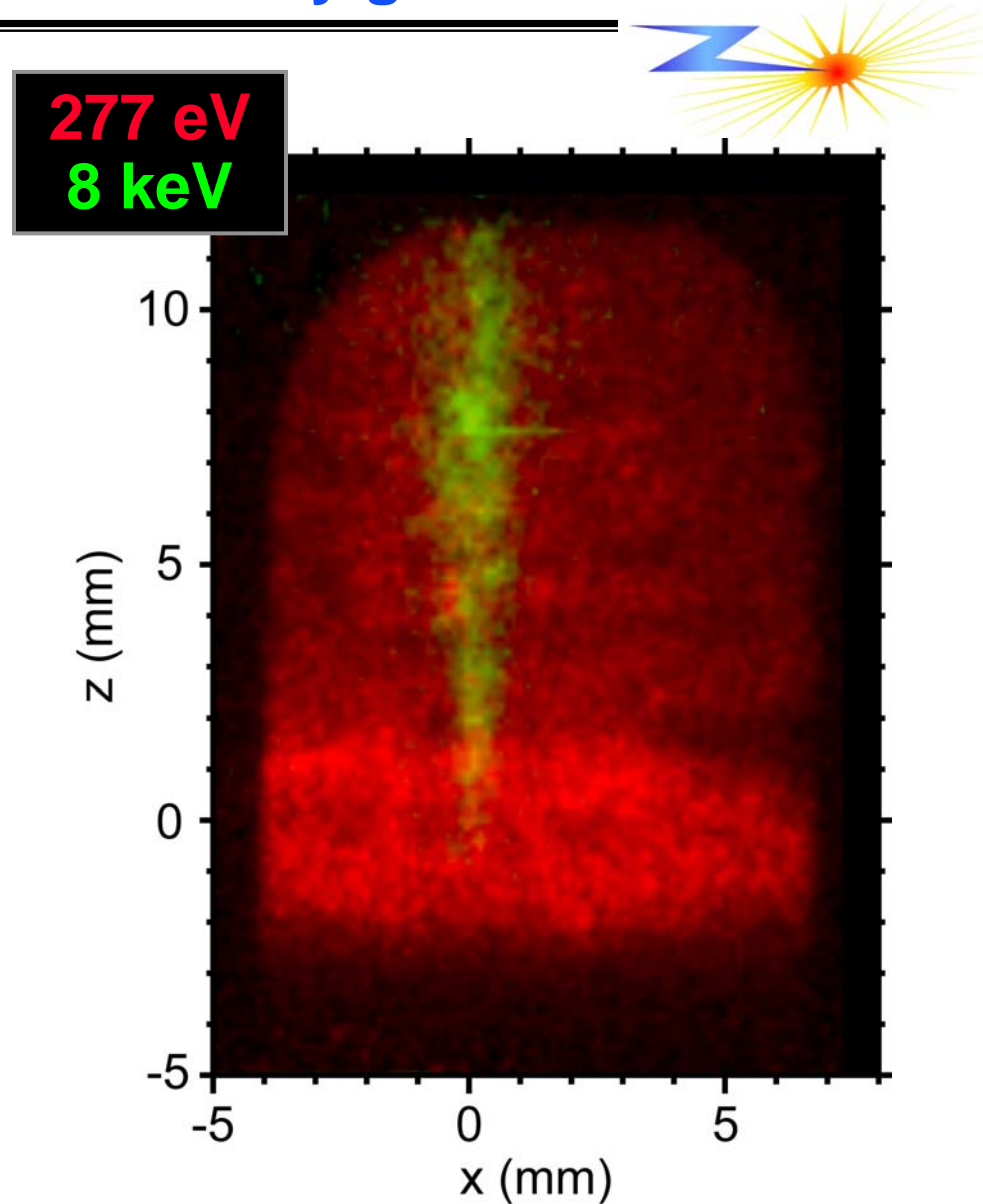
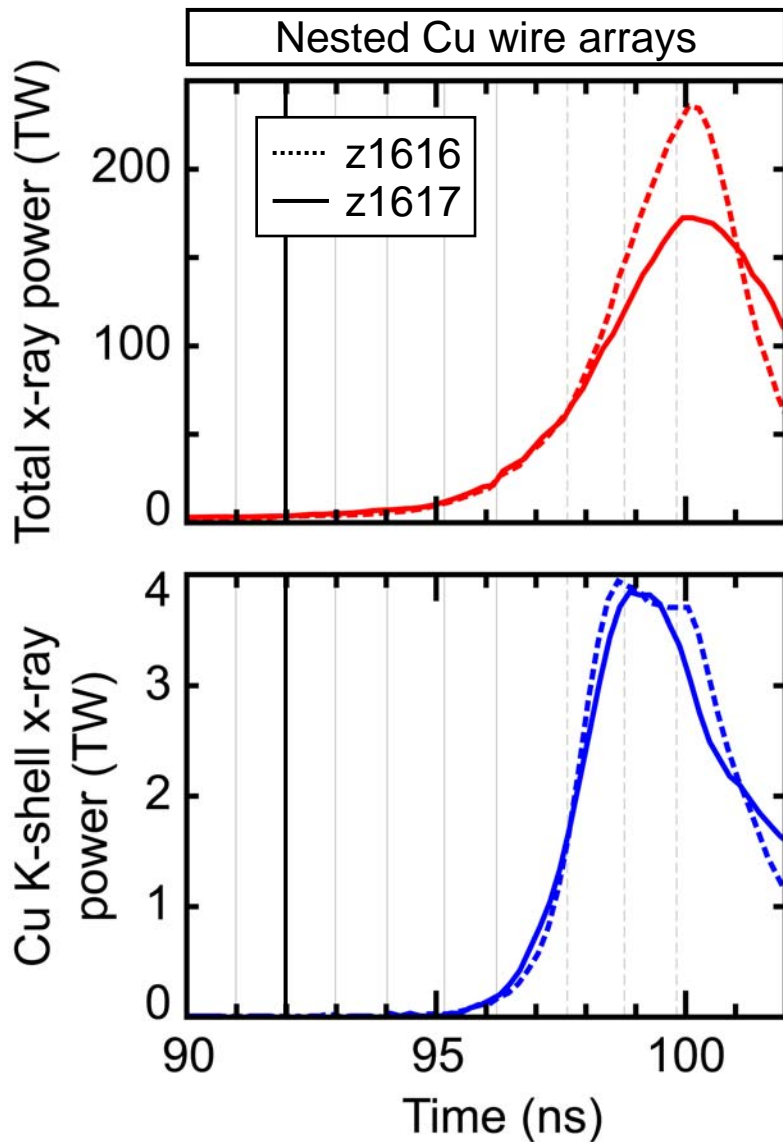
Z-pinch implosion dynamics and x-ray generation studied



Sandia
National
Laboratories

BJ 13

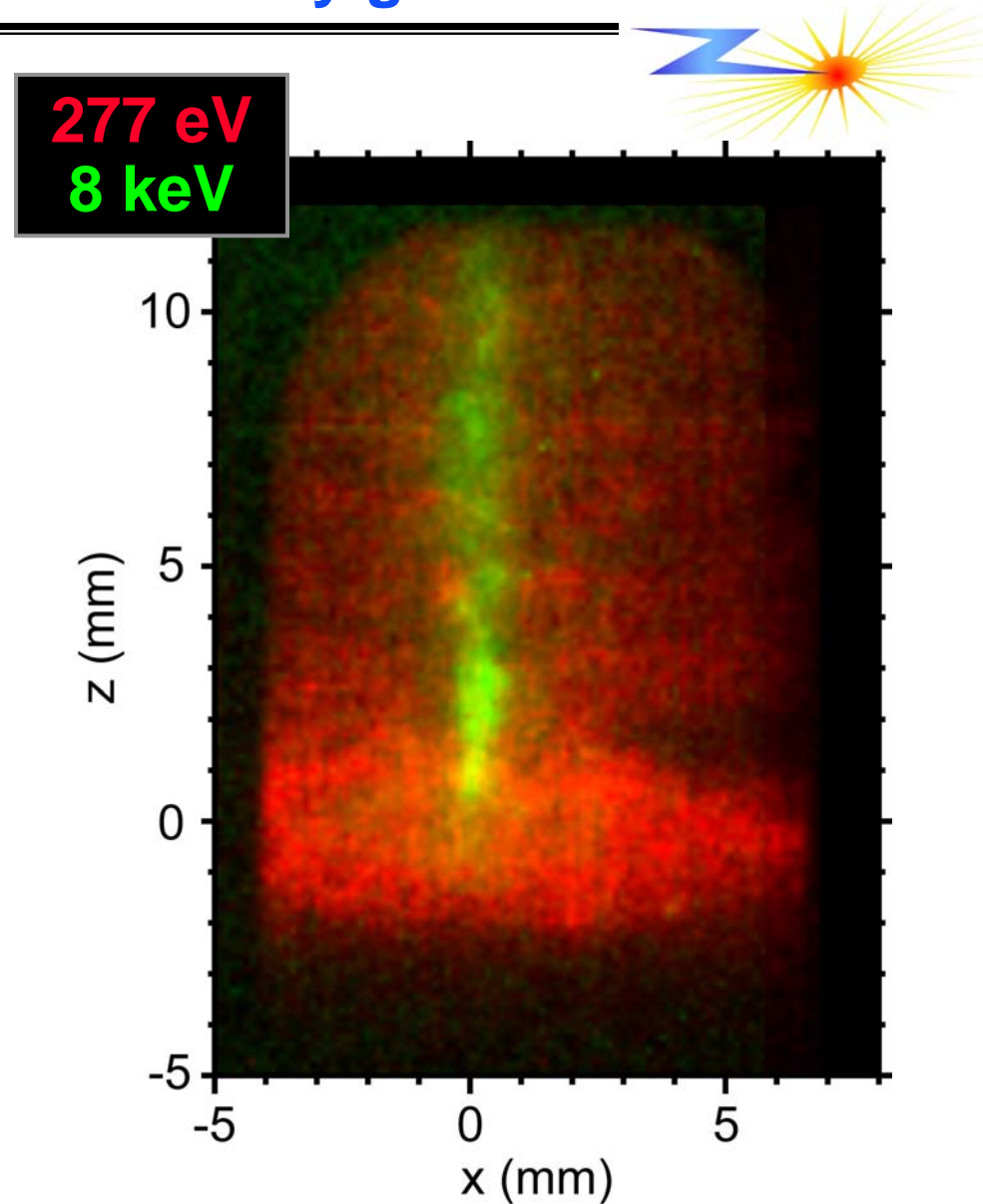
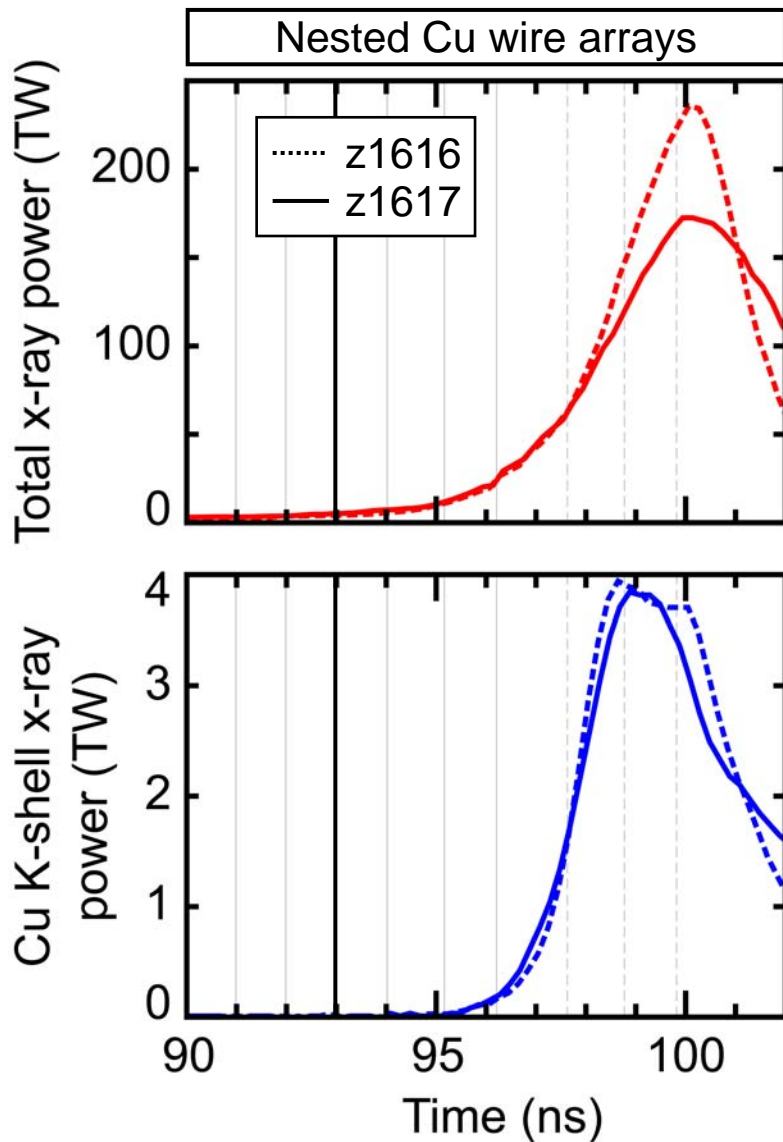
Z-pinch implosion dynamics and x-ray generation studied



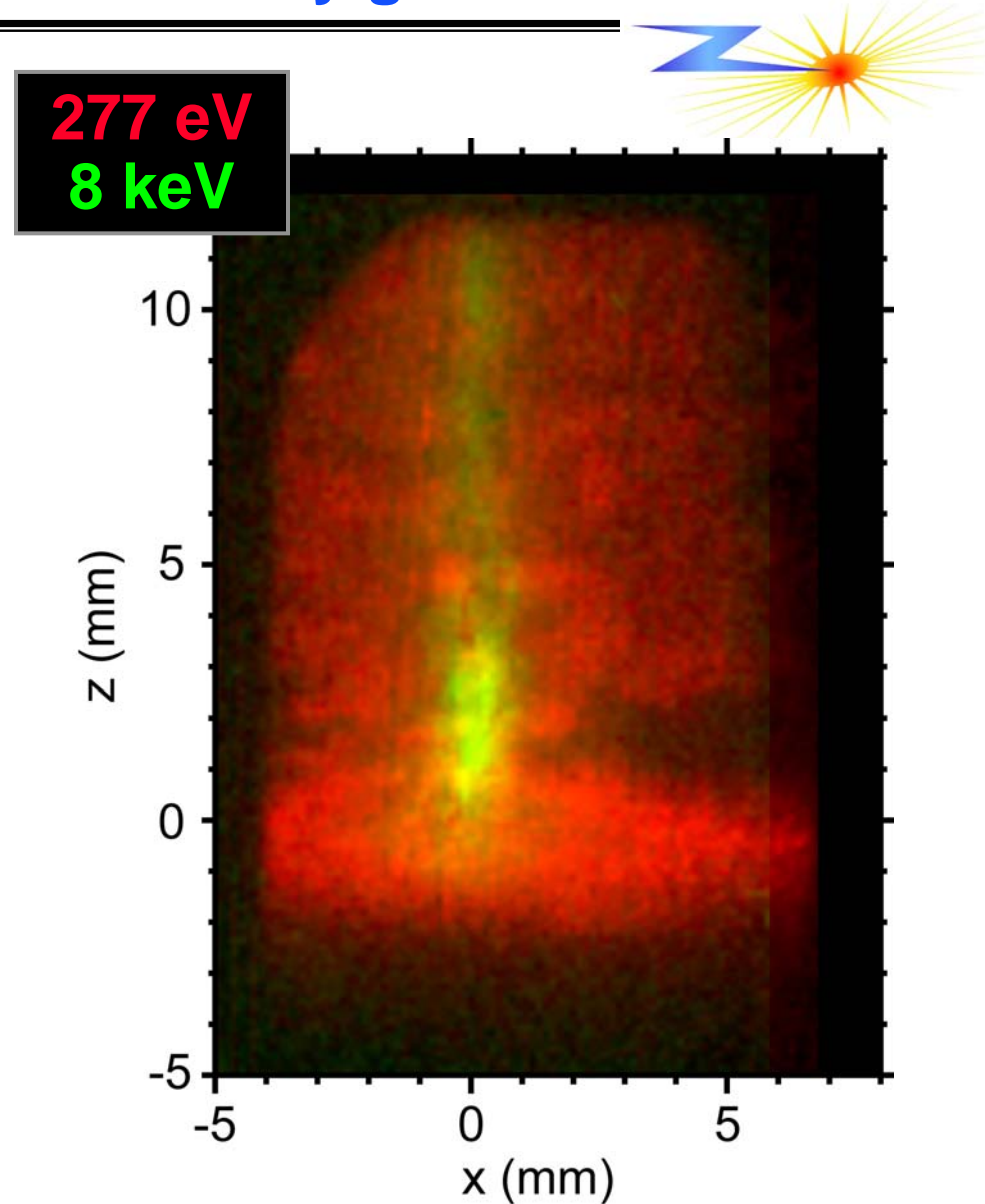
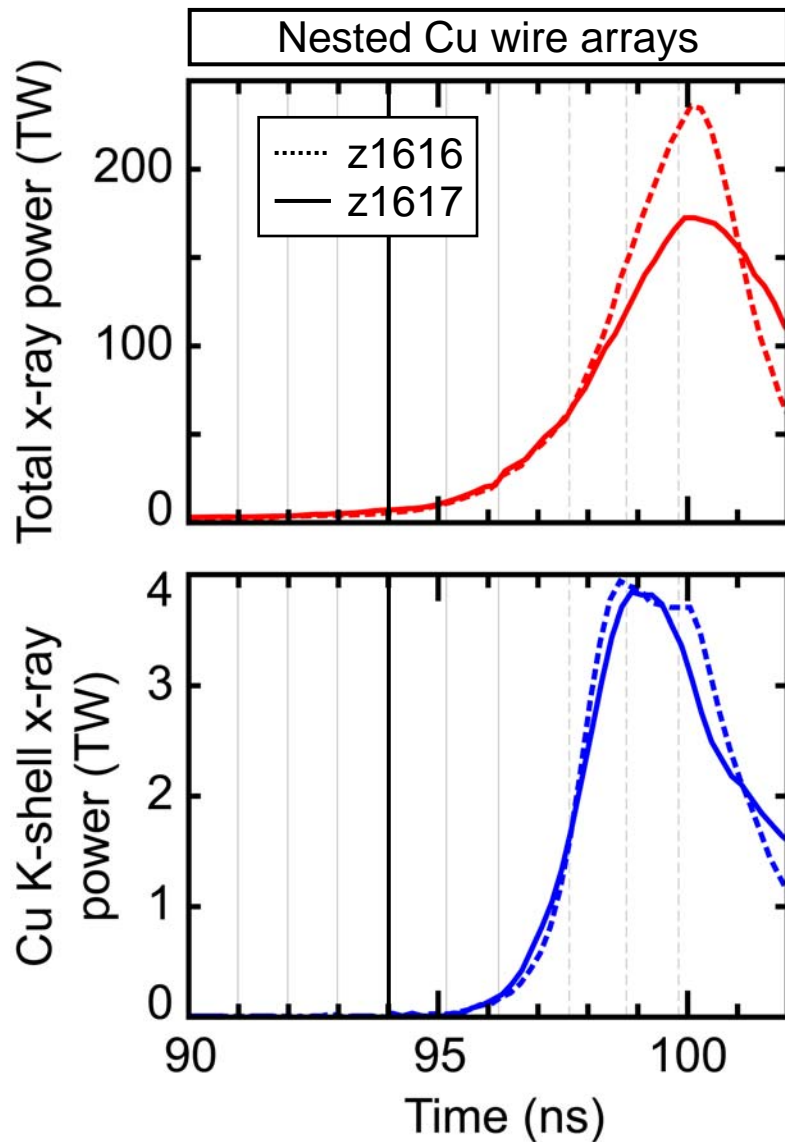
Sandia
National
Laboratories

BJ 14

Z-pinch implosion dynamics and x-ray generation studied



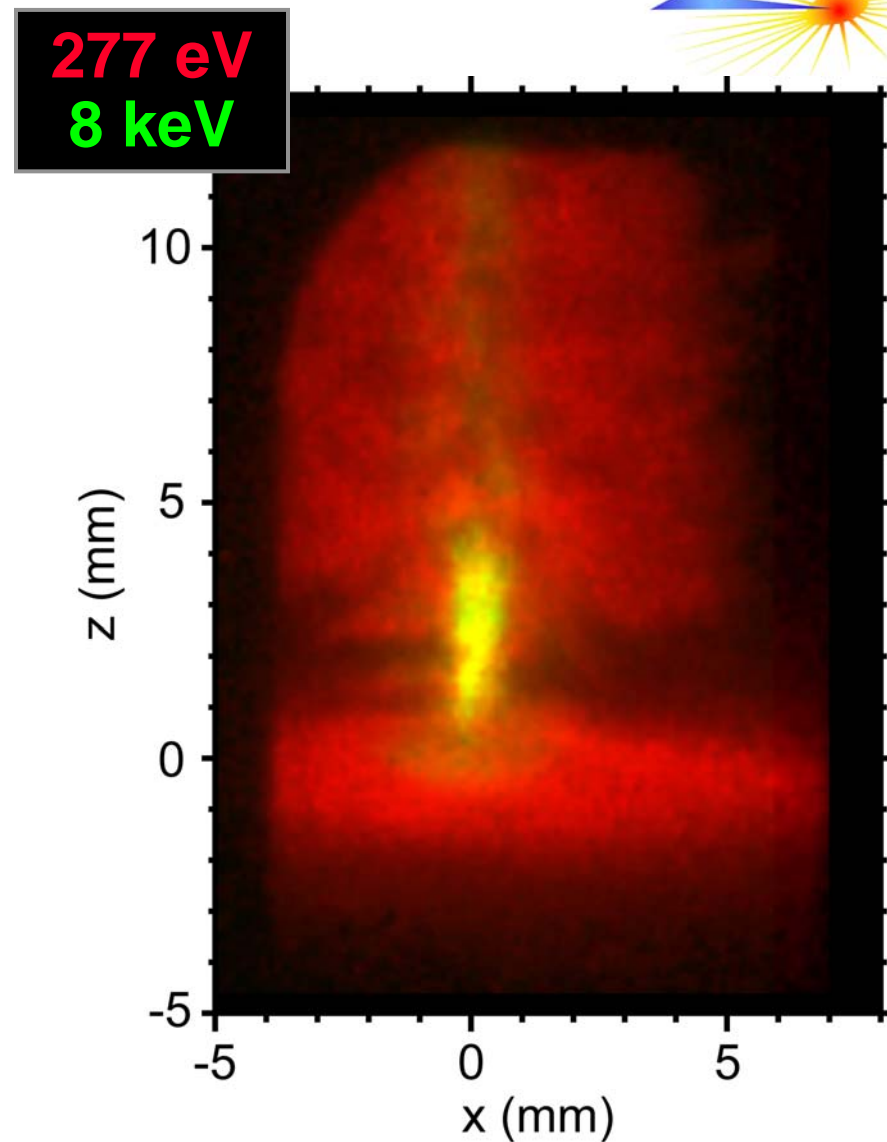
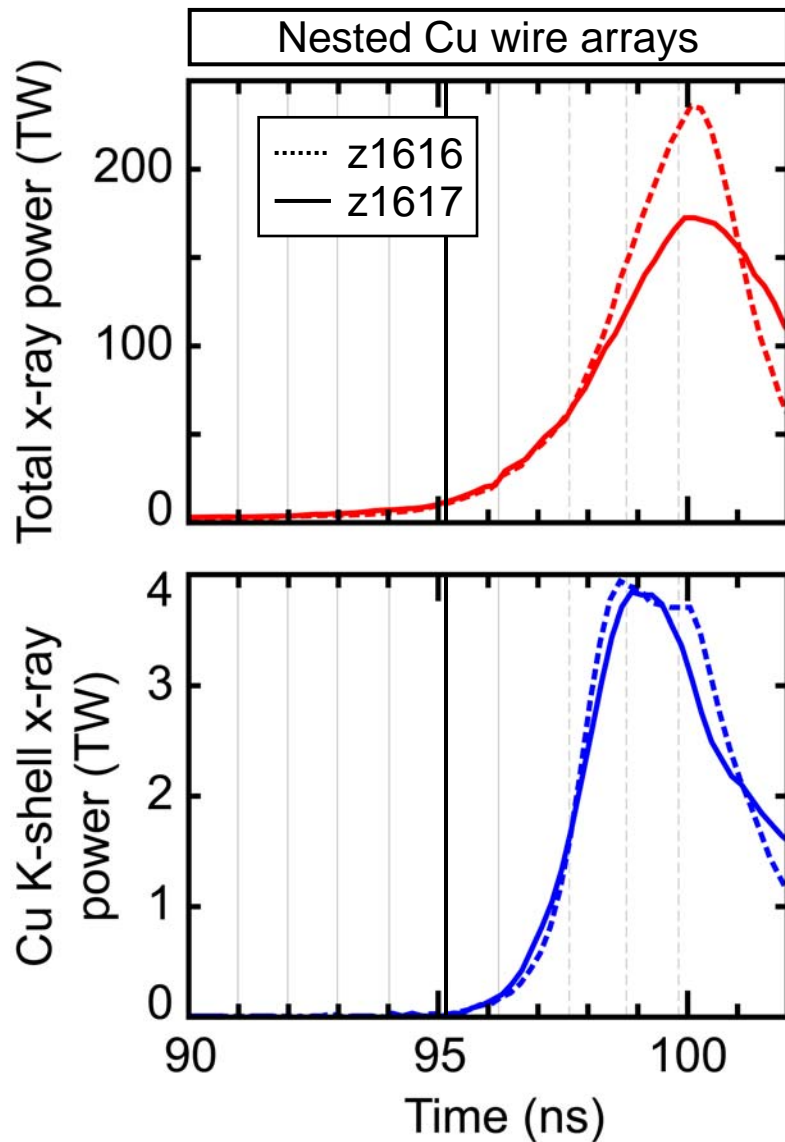
Z-pinch implosion dynamics and x-ray generation studied



Sandia
National
Laboratories

BJ 16

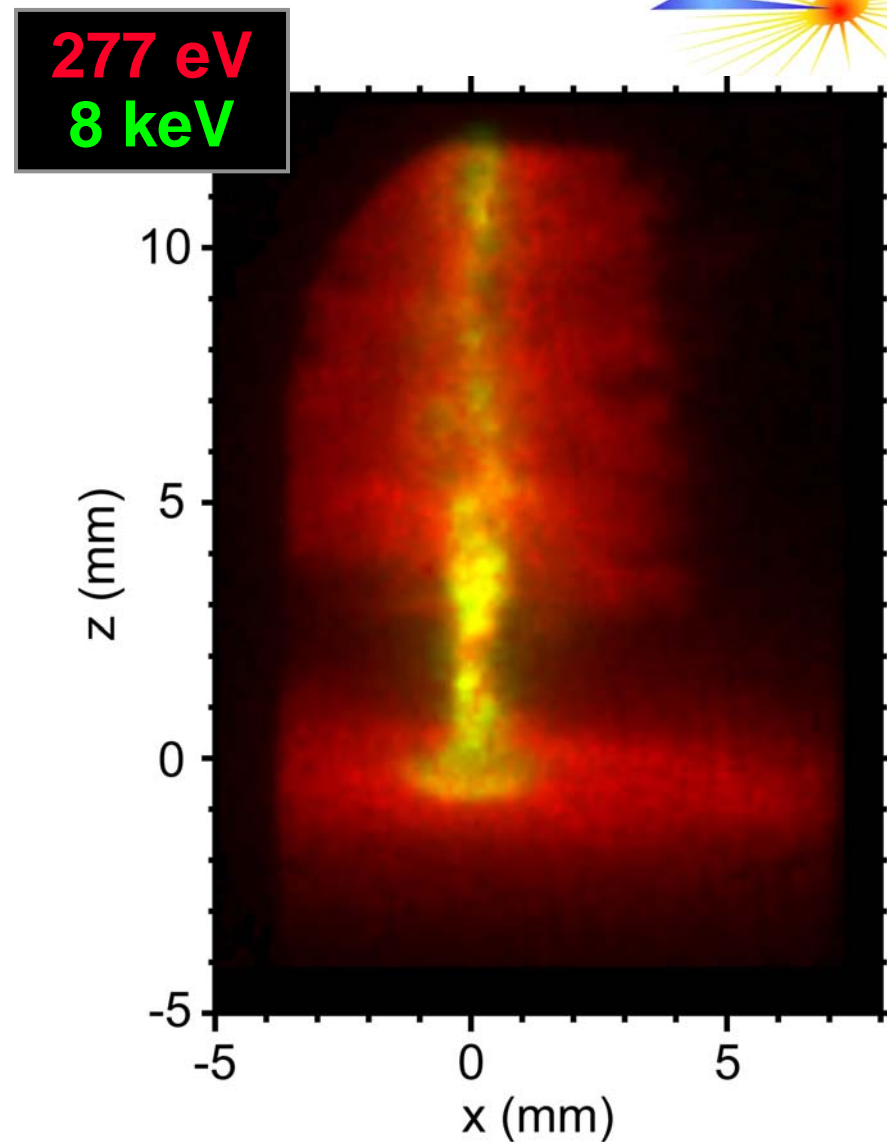
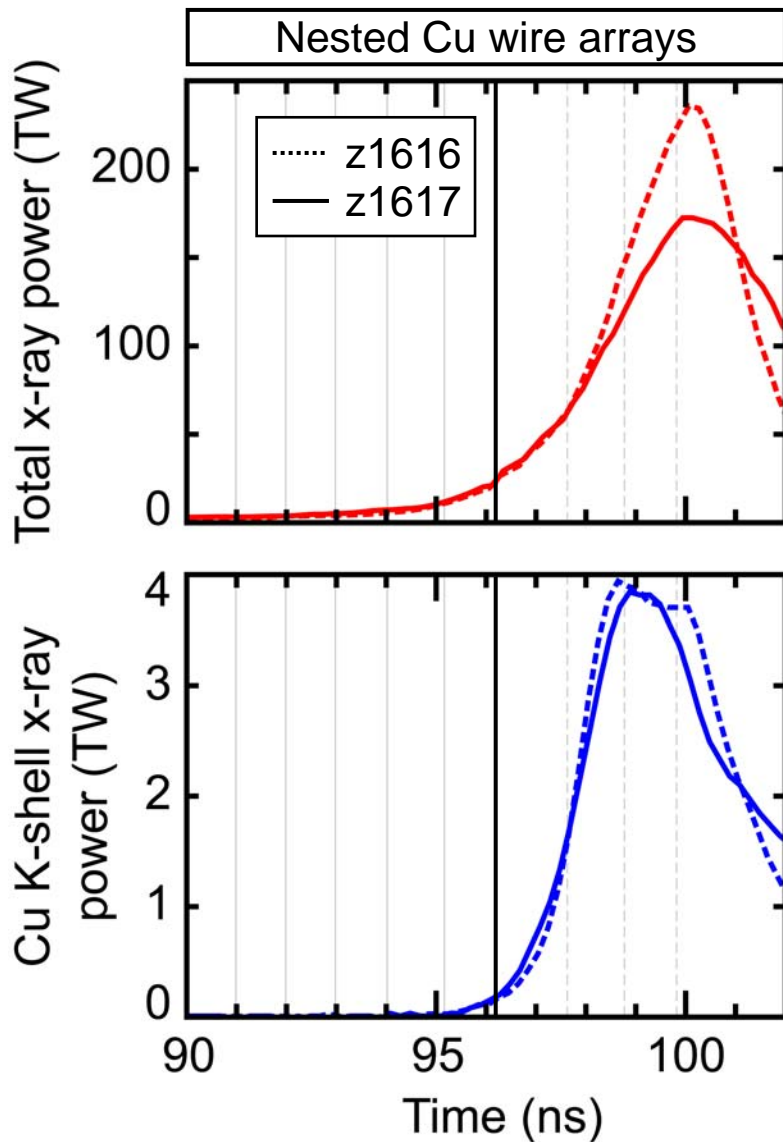
Z-pinch implosion dynamics and x-ray generation studied



Sandia
National
Laboratories

BJ 17

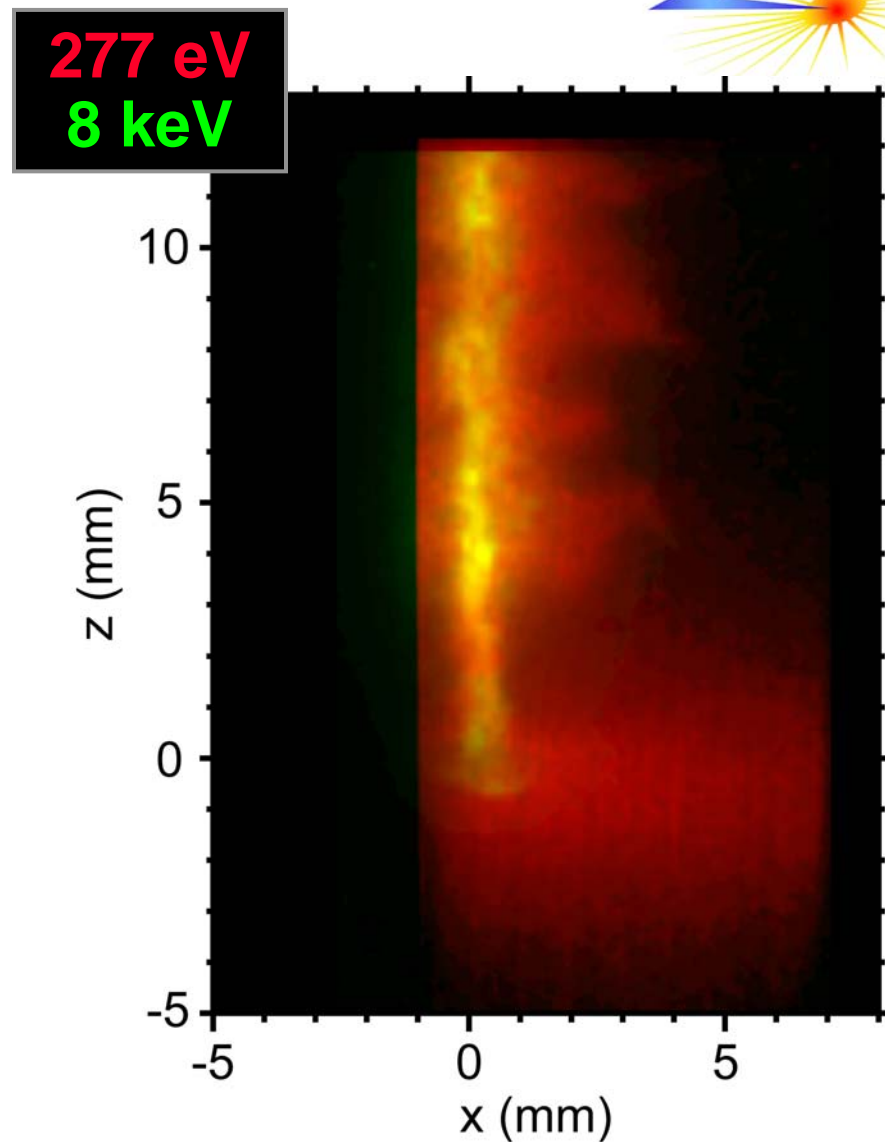
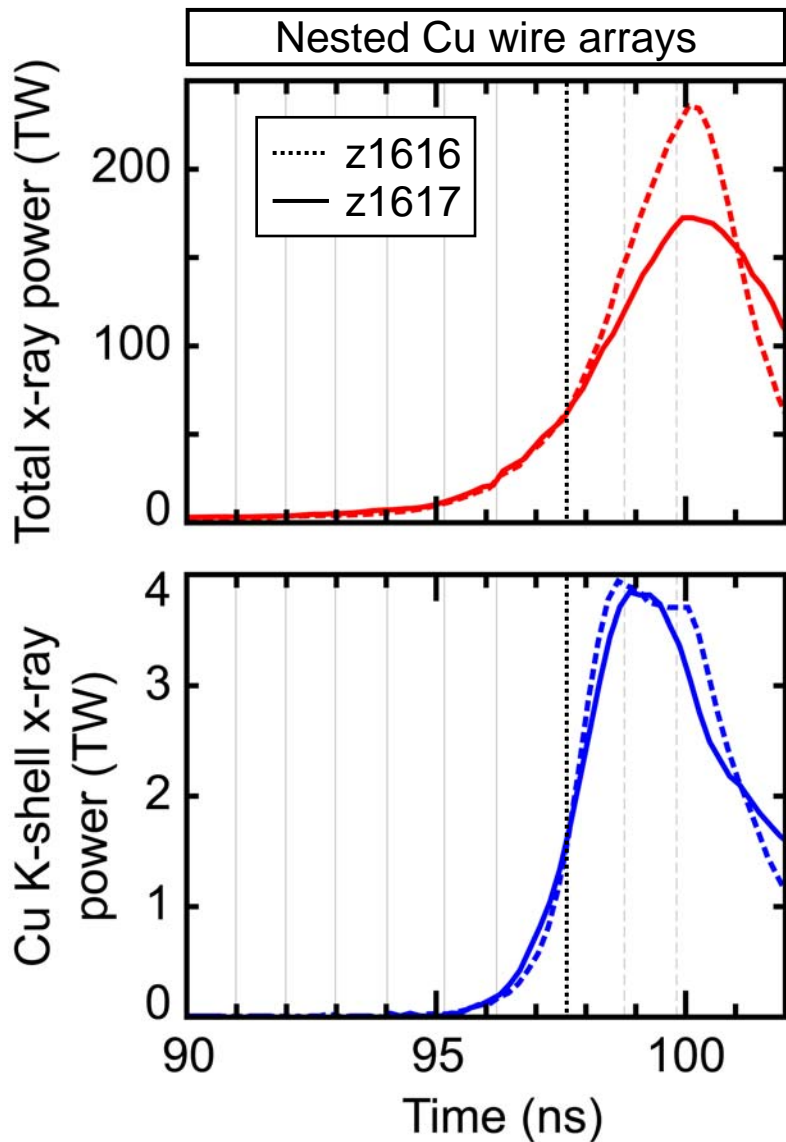
Z-pinch implosion dynamics and x-ray generation studied



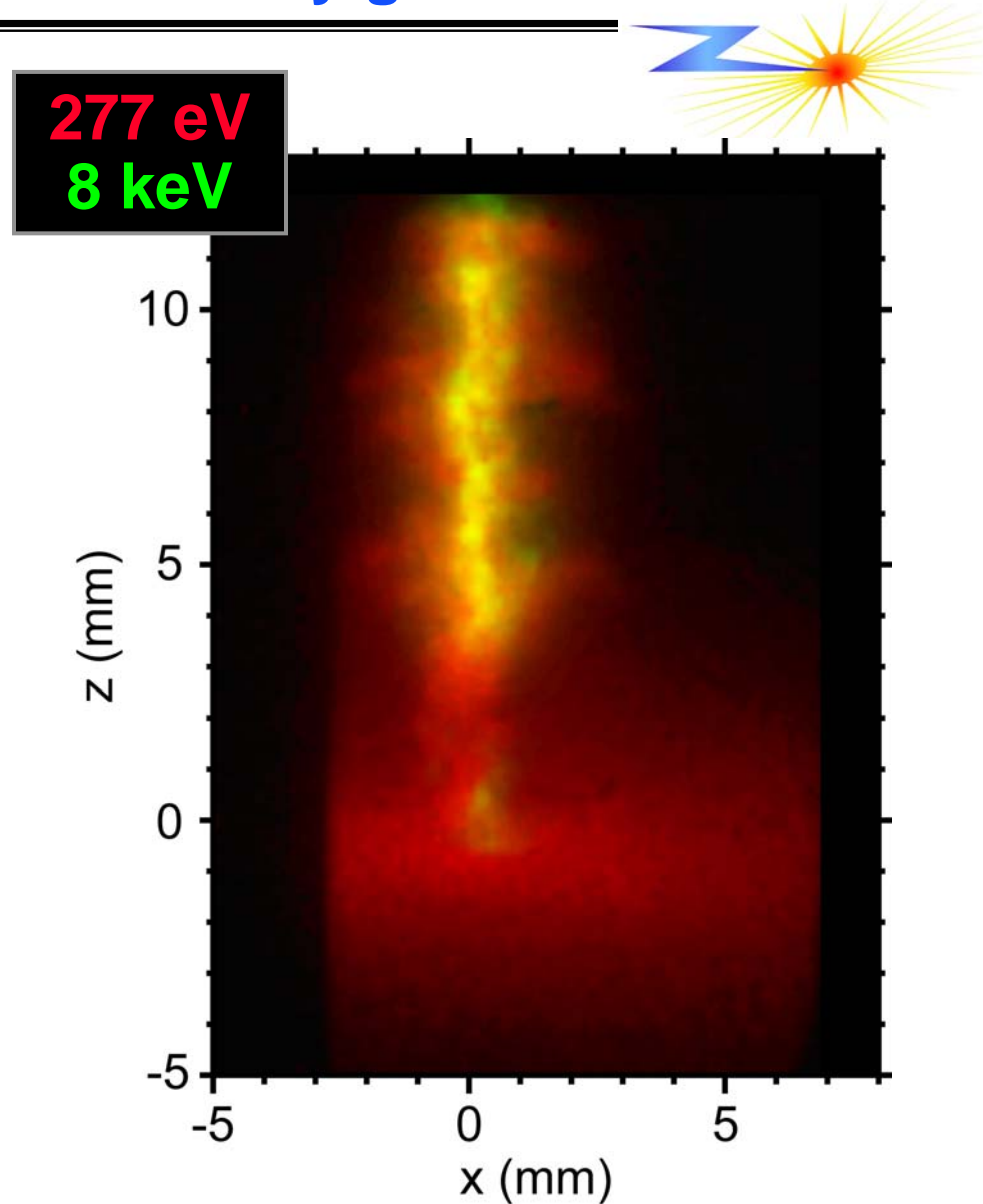
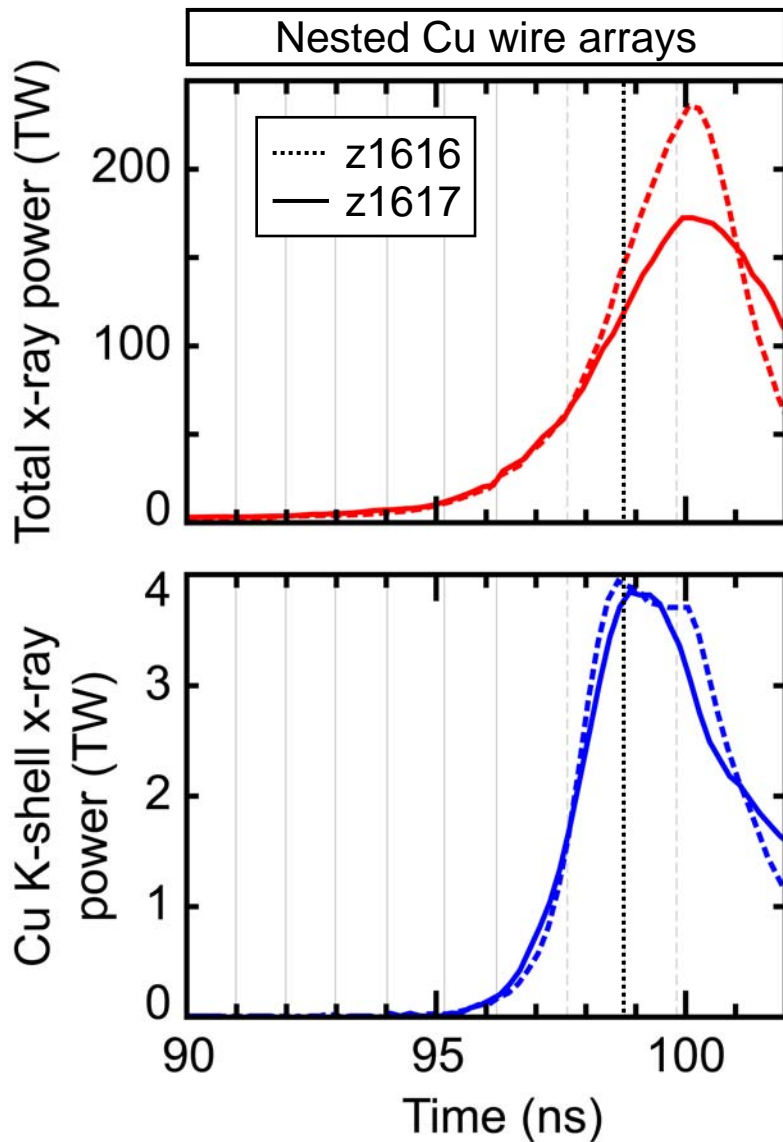
Sandia
National
Laboratories

BJ 18

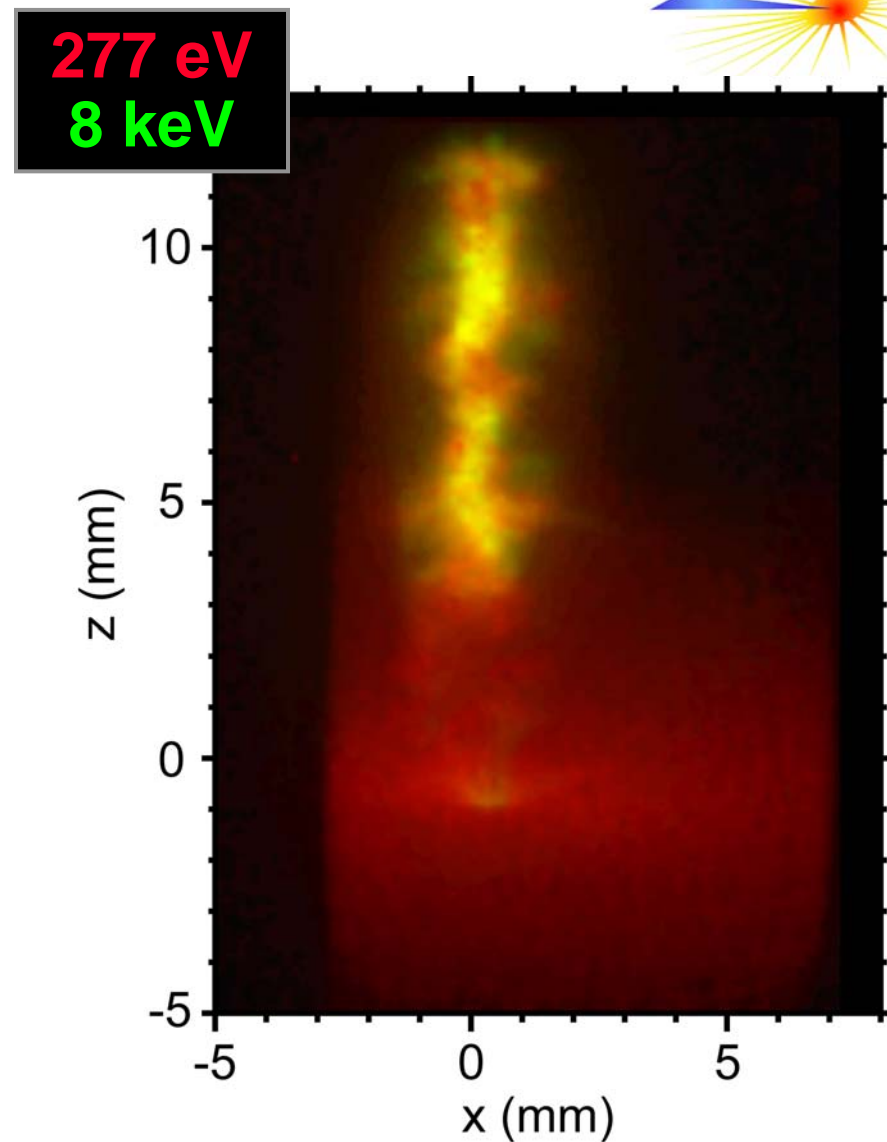
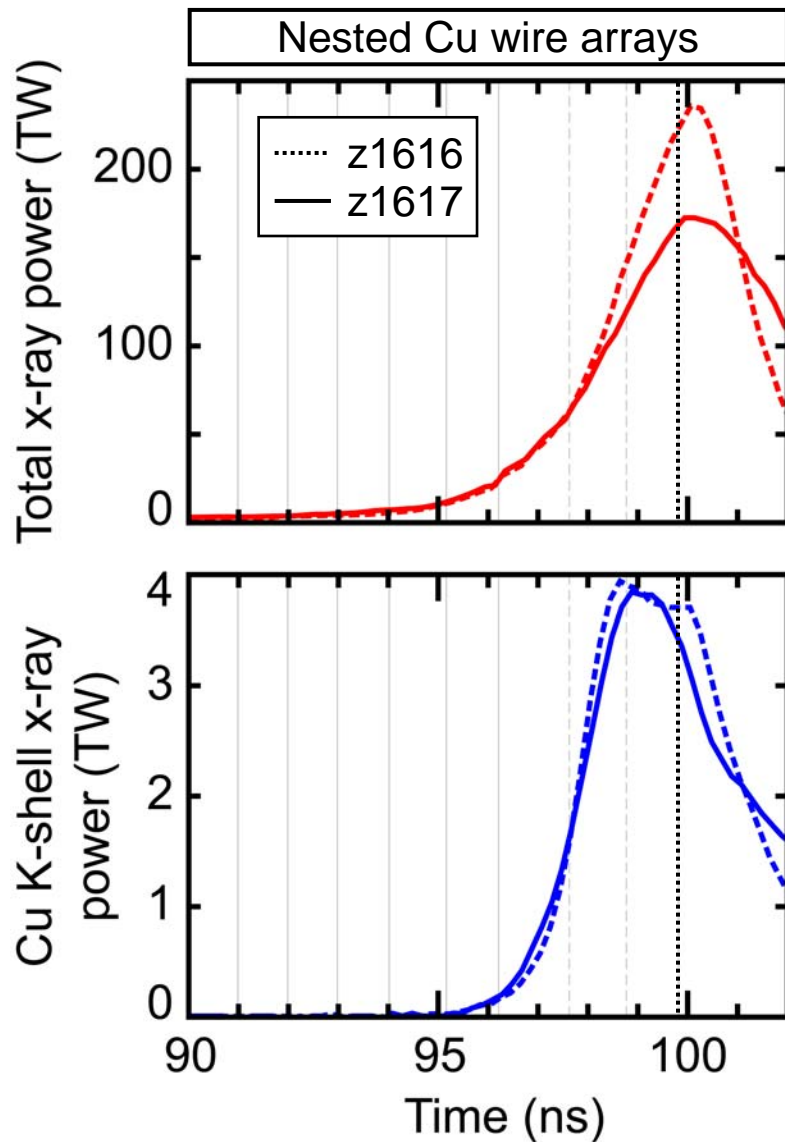
Z-pinch implosion dynamics and x-ray generation studied



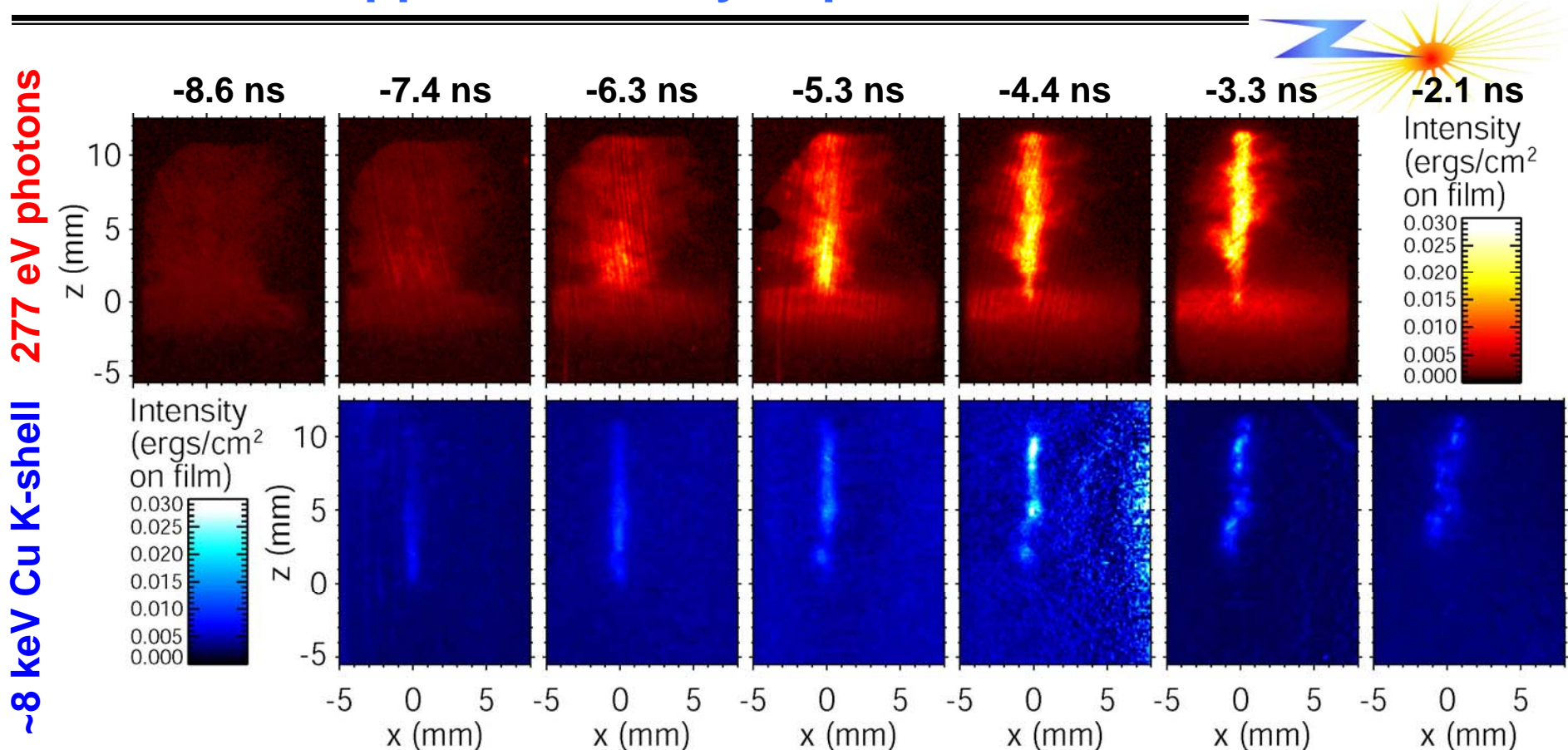
Z-pinch implosion dynamics and x-ray generation studied



Z-pinch implosion dynamics and x-ray generation studied



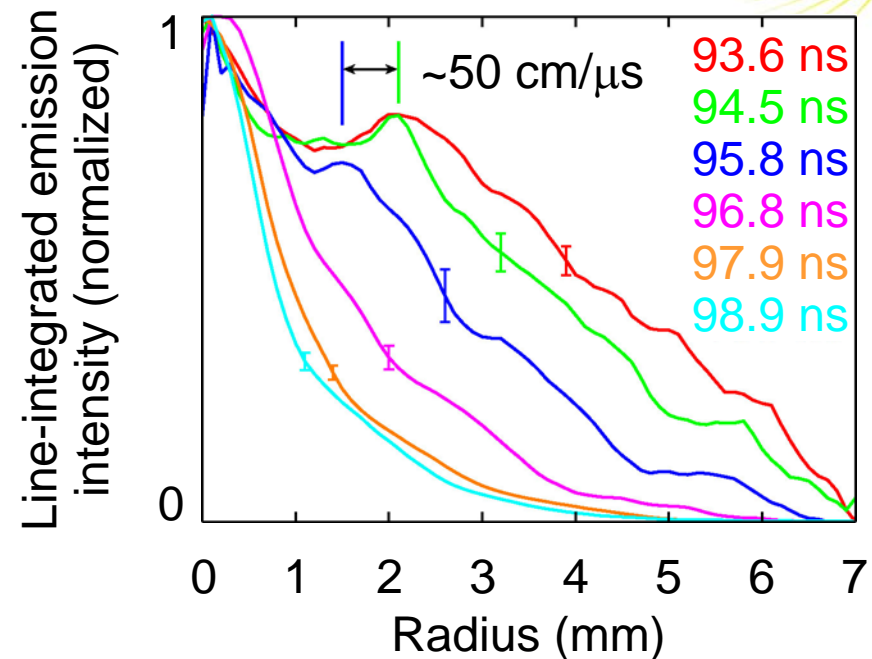
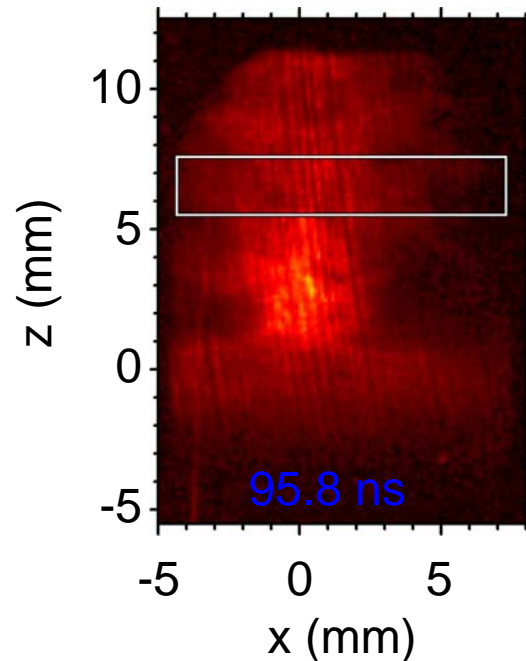
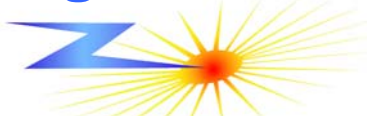
Z1436 copper wire array implosion studied in detail



- Simultaneous imaging at ~ 277 eV and ~ 8 keV Cu K-shell
- Gradual accretion of mass on axis during ~ 5 ns x-ray pulse rise
- 3D structure: zipper at stagnation, trailing mass at large radius
- No brems background on MLM-reflected images

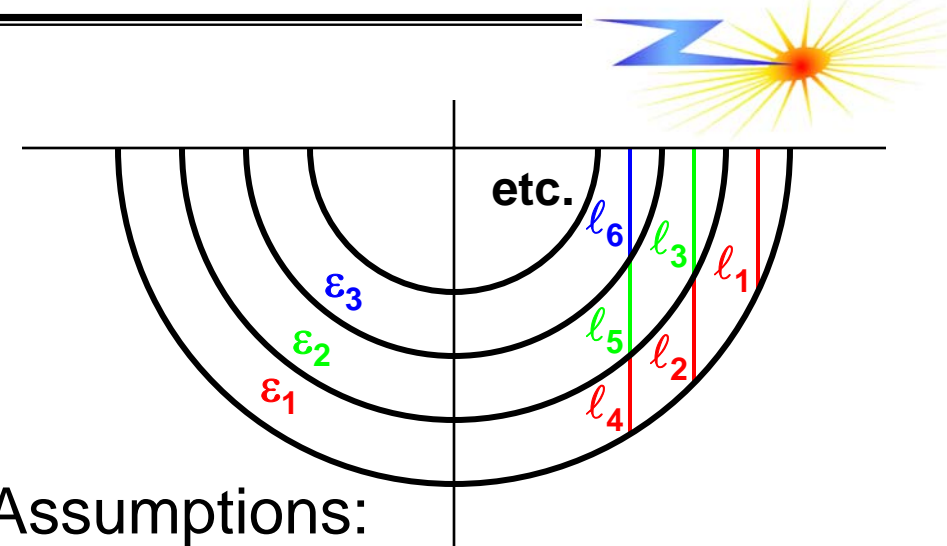
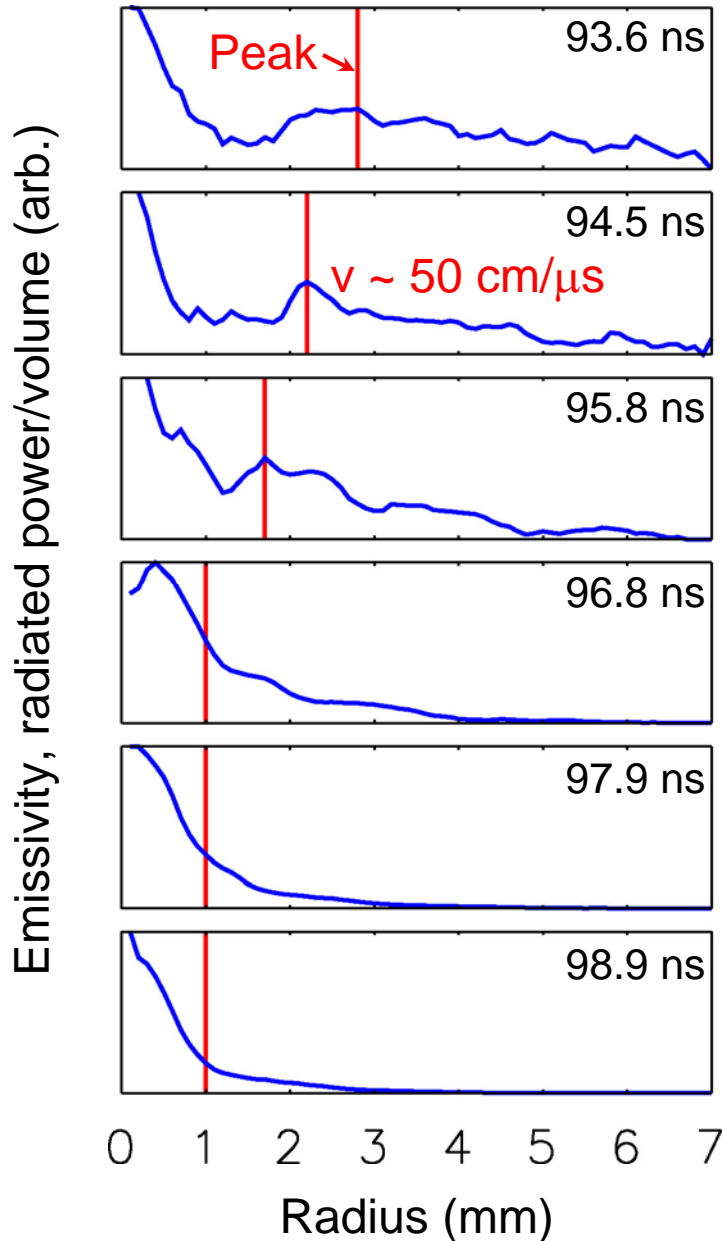
B. Jones *et al.*, IEEE T. Plasma Sci. **34**, 213 (2006).

Radial structure of imploding shell studied at stagnation



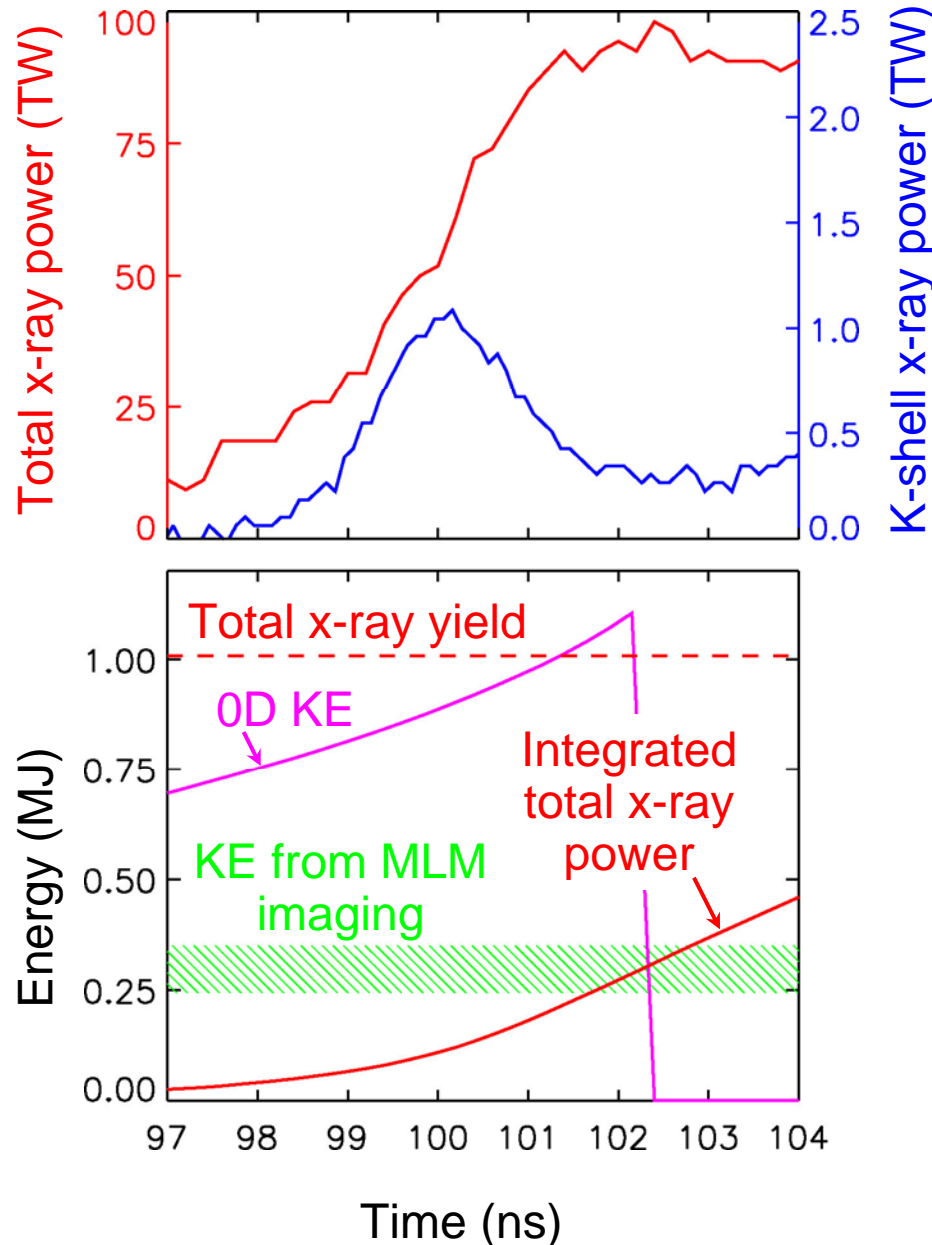
- Radial line-out taken across each 277 eV image
 - Average over axial structure, above cathode zipper and re-emission
 - Smoothed corresponding to 480 μm camera resolution
 - Error bars represent asymmetry from left to right of axis
- A diffuse shell appears to implode onto a column on axis
 - 60 cm/μs shell velocity \ll 110 cm/μs 0D calculation
 - Presence of hollow features implies opacity is not high

Emissivity profiles inferred from Abel-inverted self-emission



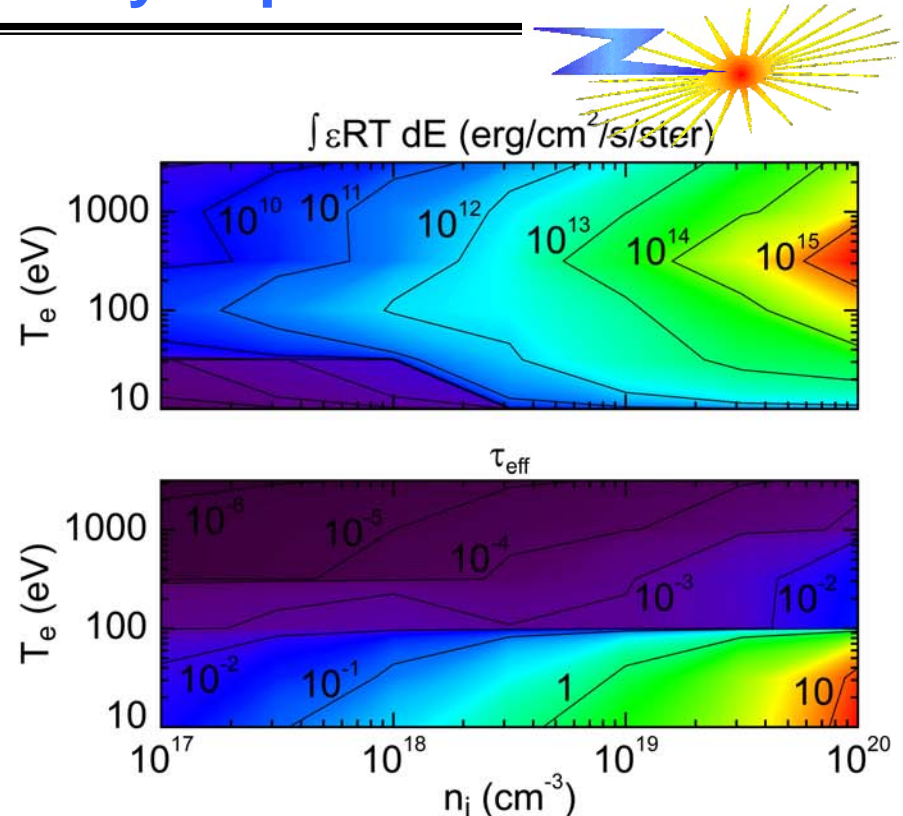
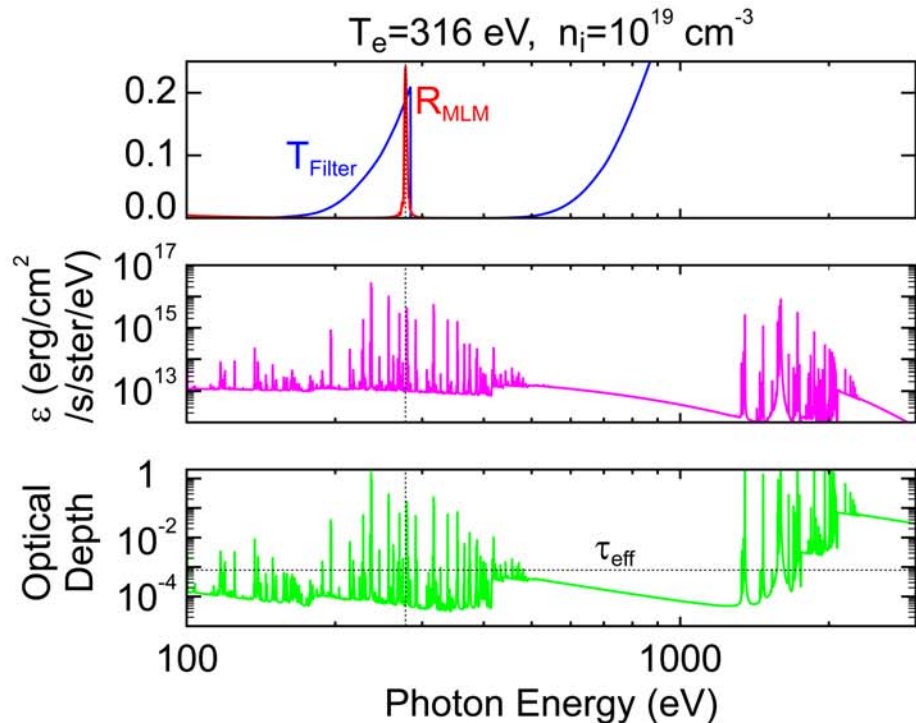
- Assumptions:
 - Emission is optically thin at 277 eV
 - Cylindrically symmetric geometry
- Numerical Abel inversion method
 - H. K. Park, Plasma Phys. Control. Fusion **31**, 2035 (1989).
- 50-60 cm/ μ s velocities, over 4-5 mm radial shell width
- $\sim 4 \text{ mm}/60 \text{ cm}/\mu\text{s} \sim 7 \text{ ns}$, equal to measured FWHM of total x-ray pulse

Estimated kinetic energy is inadequate to explain x-ray yield



- Kinetic energy is estimated assuming all of the mass is moving at 50-60 cm/μs
- KE can account for initial x-ray rise, but not total yield
- 2D and 3D MHD calculations predict $p \cdot dV$ work driven by $\mathbf{j} \times \mathbf{B}$ and Ohmic heating will dominate KE deposition
 - D. L. Peterson *et al.*, Phys. Plasmas **5**, 3302 (1998).
 - J. P. Chittenden *et al.*, Plasma Phys. Control. Fusion **46**, B457(2004).

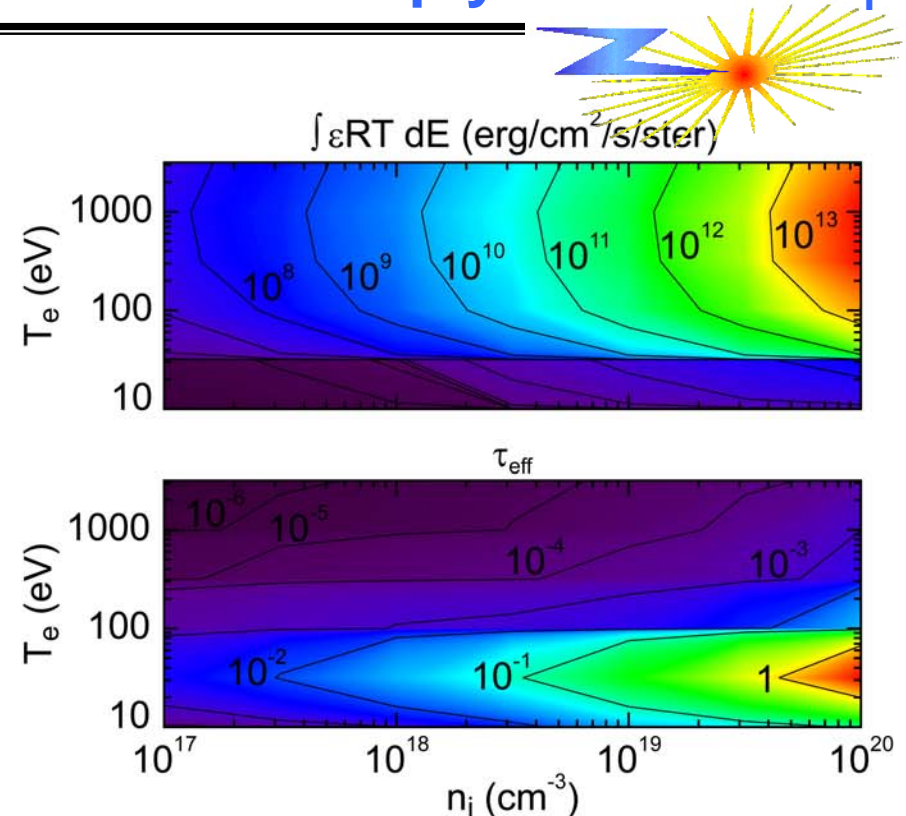
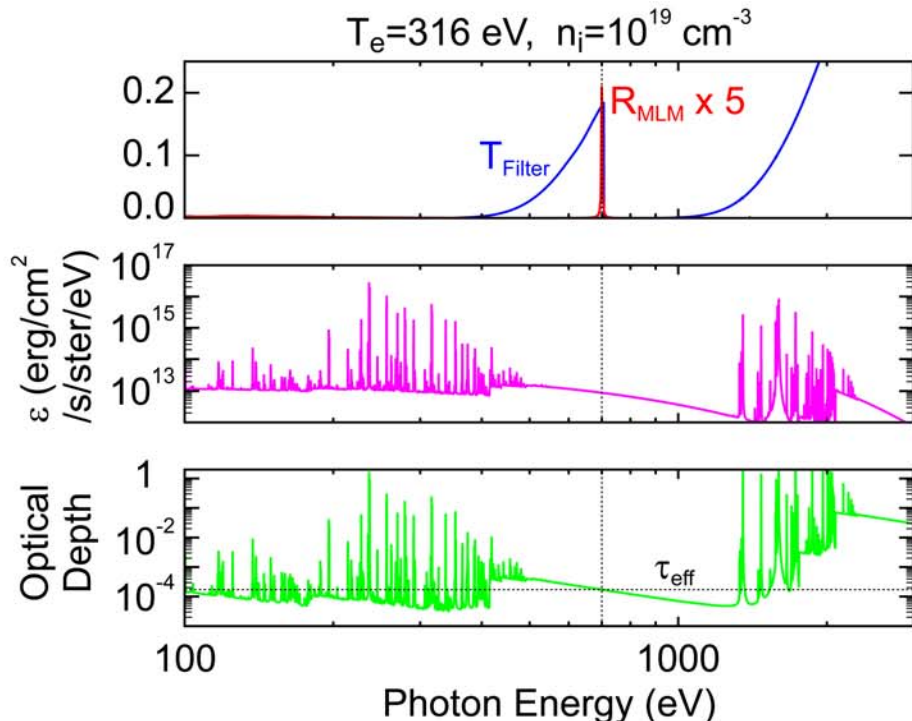
CR simulations to relate emissivity to plasma conditions



- Non-LTE PrismSPECT collisional-radiative code*
- 95% Al, 5% Mg over range of n_i , T_e
- All atomic levels for B-like through H-like; all ground state levels
- 1D radiation transport with 1 mm path length
- Optically thin emission evident for $T_e > 100$ eV

*J. J. MacFarlane *et al.*, Proc. IFSA 2003, 457 (2004).

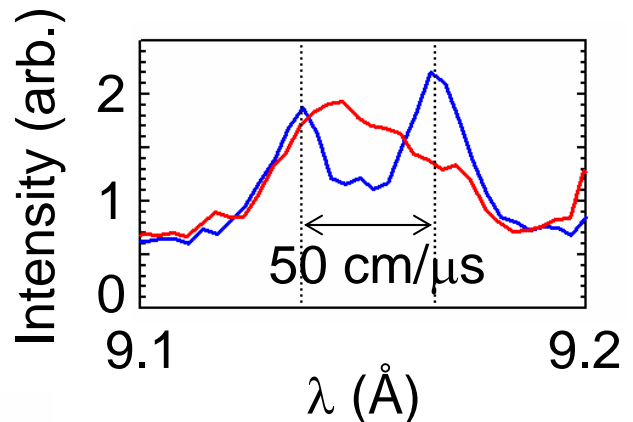
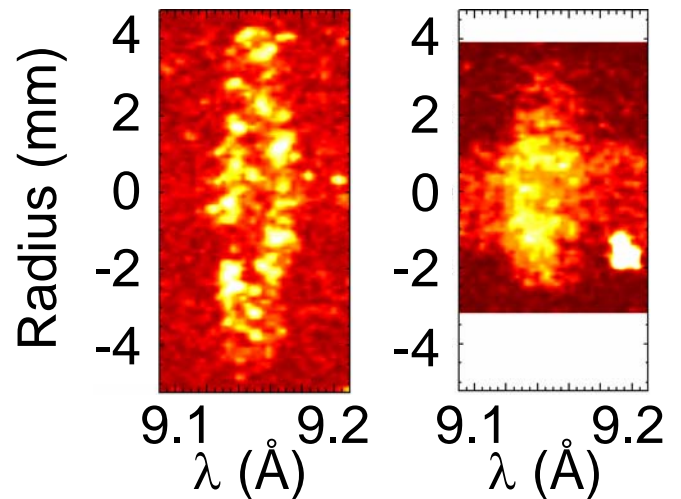
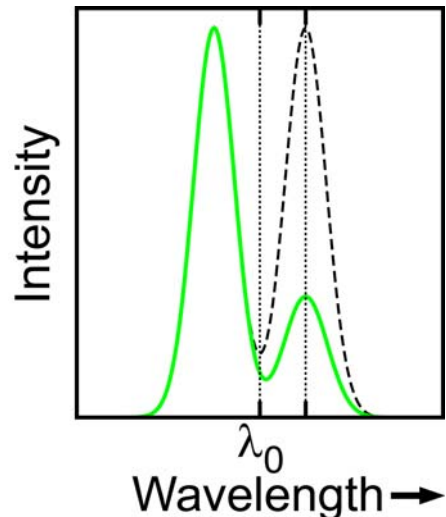
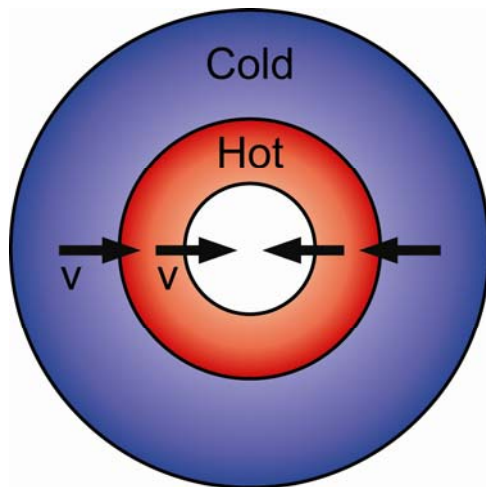
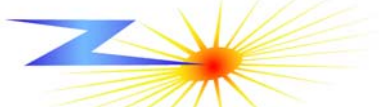
L-shell continuum imaging may be more simply related to n_i



- Non-LTE PrismSPECT collisional-radiative code*
- 95% Al, 5% Mg over range of n_i , T_e
- All atomic levels for B-like through H-like; all ground state levels
- 1D radiation transport with 1 mm path length
- Optically thin emission evident for $T_e > 100$ eV

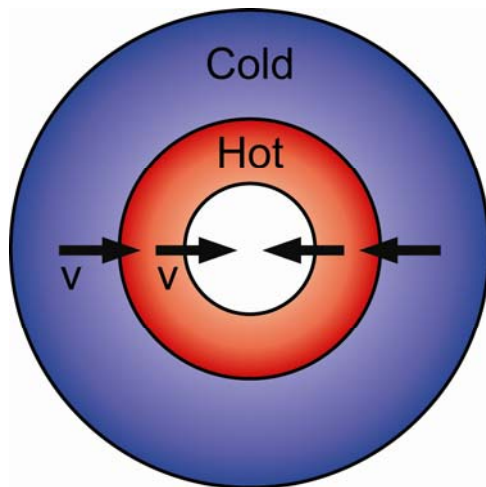
*J. J. MacFarlane *et al.*, Proc. IFSA 2003, 457 (2004).

Optically thin Doppler splitting seen in low-mass Al wire array

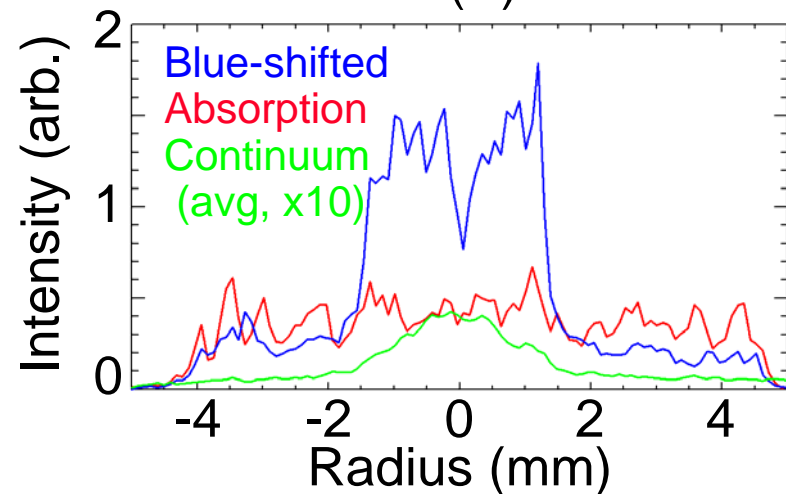
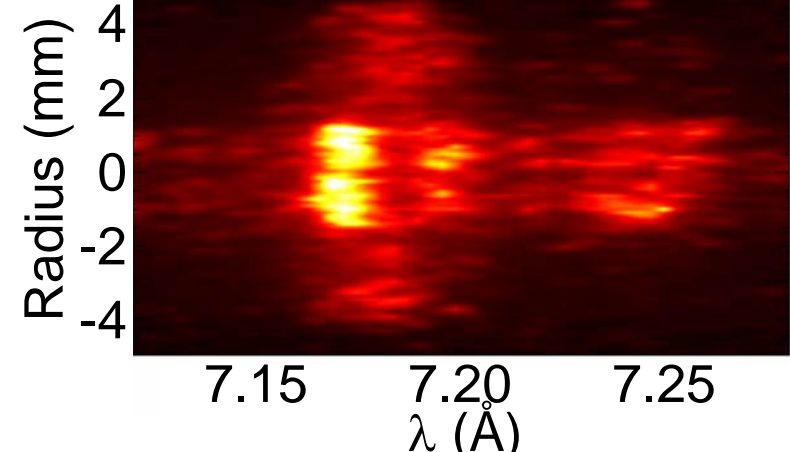
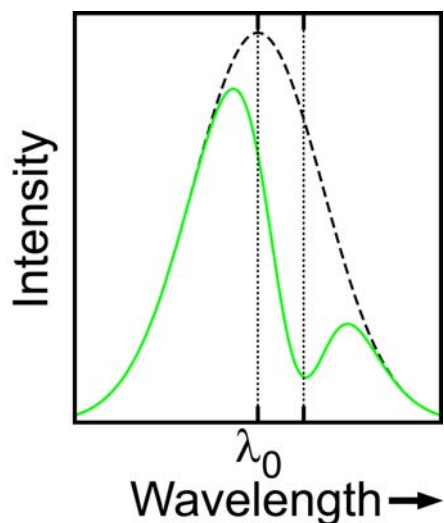
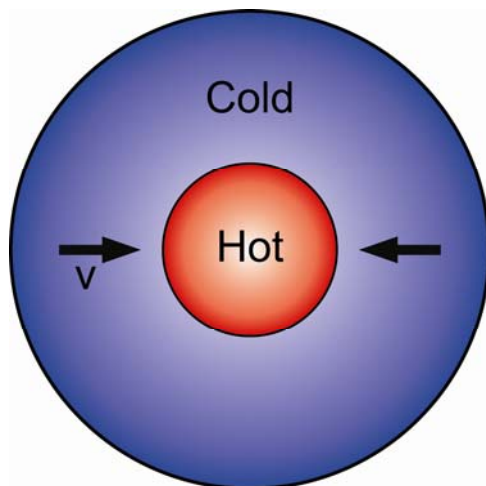
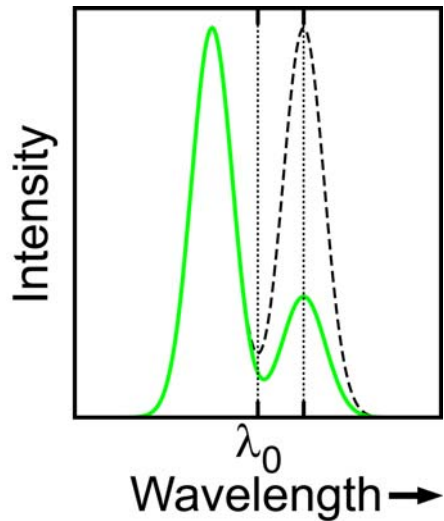


- Oval shape—Doppler split seen on axis, but not in tangential view of shell
- At early time, red/blue-shifted lines are similar magnitude \Rightarrow optically thin
- Speckle could be azimuthal structure
- At later times, red-shifted line is attenuated by shell/trailing mass opacity
- Splitting not so obvious in Al lines—brighter precursor emission on axis?

Doppler-shifted absorption seen in high-mass Al wire array



Opacity in cold trailing mass

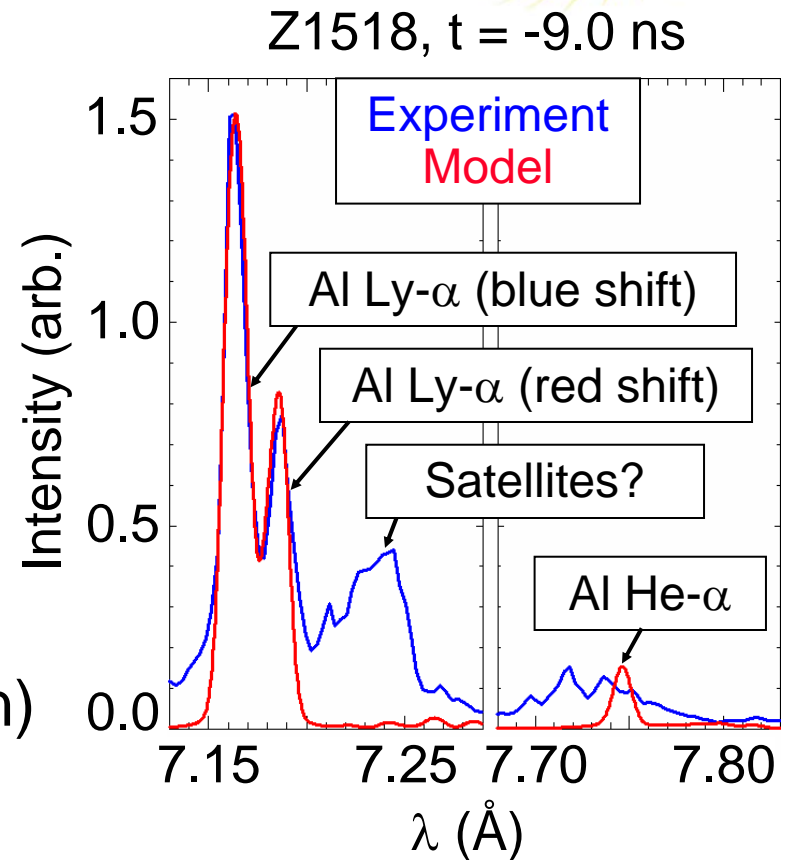
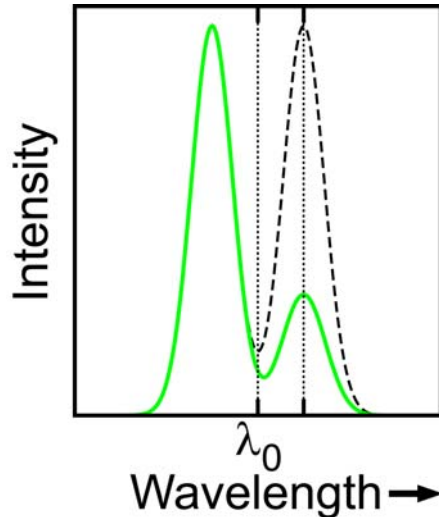
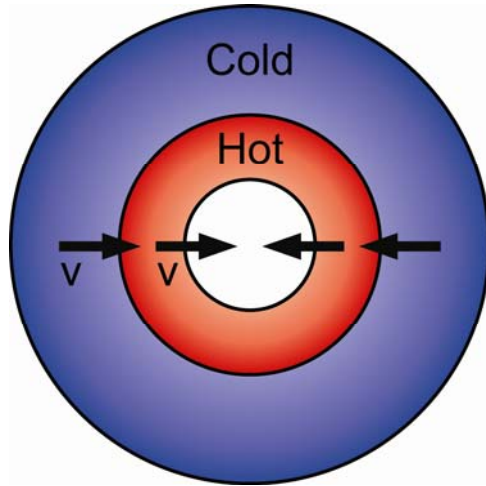


Sandia
National
Laboratories

Doppler-shifted absorption seen in high-mass Al wire array



Opacity in cold trailing mass attenuates red-shifted Al Ly- α and He- α



- Collisional-radiative model, radiation transport in discrete zones (Y. Maron)
 - Hot: $1.5 \text{ mm} < R < 2 \text{ mm}$
 - Cold: $2 \text{ mm} < R < 9 \text{ mm}$
- Line shape calculations
 - Stark broadening (not dominant)
 - Doppler broadening/splitting (implemented for first time, $\delta v/v=10\%$)
- Preliminary results (need to consider satellites):
 - Hot: $n_i = 5 \times 10^{19} \text{ cm}^{-3}$, $T_e = 700 \text{ eV}$, $v = 40 \text{ cm}/\mu\text{s}$
 - Cold: $n_i = 5 \times 10^{19} \text{ cm}^{-3}$, $T_e = 150 \text{ eV}$, $v = 30 \text{ cm}/\mu\text{s}$

Summary



- Abel inversion yields physically relevant information despite deviation from cylindrical symmetry
- Continuity equation approach offers a technique for inferring plasma momentum and kinetic energy
- Several independent possibilities for measuring density profiles
- Spectroscopic techniques can offer independent velocity measurement, and plasma n , T information (especially in stagnated pinch)
- Temperature profiles are needed in addition to say more about compressional heating, thermalization rates, energy partitioning, etc.